

Origin and tectonic significance of corundum–kyanite–sapphirine amphibolites from the Variscan French Massif Central

J. BERGER,^{1*} O. FÉMÉNIAS,¹ D. OHNENSTETTER,² G. PLISSART^{1†} AND J.-C. C. MERCIER³

¹Département des Sciences de la Terre et de l'Environnement – CP 160/02, Université Libre de Bruxelles (ULB), 50 Avenue Roosevelt, B-1050 Brussels, Belgium (juberger@ulb.ac.be)

²CNRS, Centre de Recherches Pétrographiques et Géochimiques, B.P. 20, F-54501 Vandoeuvre-lès-Nancy Cedex, France

³UMR CNRS 6250 'LIENSs', ILE, Université de la Rochelle, 2 rue Olympe de Gouges F-17042 La Rochelle Cedex 1, France

ABSTRACT The contact zone between two major allochthonous lithotectonic units in the French Massif Central (FMC) is characterized by the presence of corundum-bearing amphibolites associated with serpentinites, fiaser-gabbros, eclogites and granulites. These unusual amphibolites are best preserved in the Western FMC, where they are found within the lower oceanic crust of the Limousin ophiolite. Mineralogical observations and thermodynamic modelling of the spinel–corundum–sapphirine–kyanite amphibolites in the CMASH system show that they were formed at peak P – T conditions around 800 °C/10 kbar in response to near isothermal burial followed by a retrogressive anticlockwise path. Metamorphic reactions are controlled both by modification of P – T conditions and by local chemical changes linked to fluid infiltration. Pargasite growth has been enhanced by infiltration of Ca- and Al-rich fluids whereas kyanite- and sapphirine-forming reactions are partly controlled by local inputs of MgO–SiO₂ components, most probably during infiltration metasomatism. By analogy with worldwide ophiolites (Oman, Tethyan, Appalachian) and published numerical models, subduction of a still-hot oceanic ridge is proposed to form these Al-rich amphibolites from plagioclase-rich troctolites. The trace-element composition of high-Ti, fine-grained amphibolites (former fine-grained Fe–Ti gabbros) adjacent to the corundum-bearing ones, further indicates that the oceanic crust was initially created at a mid-ocean ridge (rather than within a back-arc basin), followed by the emplacement of supra-subduction zone-type magmas, probably due to intraoceanic subduction close to the ridge.

Key words: anticlockwise path; corundum amphibolites; ophiolite; ridge subduction; Variscan.

INTRODUCTION

The subduction of oceanic slabs produces a wide range of rock types due to the different possible P – T paths and to the chemical heterogeneity of the slab constituents. Recent studies have demonstrated that the rate of burial controls the geothermal gradient along slab surfaces (Iwamori, 2000; Uehara & Aoya, 2005), but it is now well established that the P – T path of a subducting slab also largely depends on the age of the slab portion subducted, hence, on the distance of this portion to the mid-oceanic ridge (Peacock, 2003). In particular, high-temperature conditions (i.e. those corresponding to the HT amphibolite facies or to the granulite facies) are expected in the case of subduction of a young and hot oceanic lithosphere (Peacock *et al.*, 1994; Searle & Cox, 2002; Garcia-Casco *et al.*, 2008). Consequently, eclogites and blueschists are not the only markers of fossil subduction zones, and the P – T path of HP granulites and HT–HP amphibolites cropping out in orogenic belts has also to be deter-

mined precisely to constrain the pre-collisional geodynamic evolution of an orogenic belt.

One problem is that basic rocks do not always record the P – T conditions undergone by the slab as fluids and deformation are necessary media to enhance metamorphic reactions (Rubie, 1986; de Ronde & Stunitz, 2007; Schneider *et al.*, 2007; Glodny *et al.*, 2008). In the Limousin ophiolite [western French Massif Central (FMC); Dubuisson *et al.*, 1989], most rocks have preserved their oceanic characteristics (i.e. mineral assemblages and compositions), but a few corundum-bearing amphibolites have been formed under HT–HP conditions in restricted zones of fluid percolation. These corundum amphibolites are not unusual in the FMC (see Forestier & Lasnier, 1969) and they are always associated with a major tectonic suture zone, together with a wide range of mafic rocks that underwent various P – T conditions (granulites, eclogites, amphibolites and unmetamorphosed gabbros). This study presents results from mineralogical, thermodynamic and geochemical investigations to unravel the metamorphic evolution and the tectonic setting of corundum amphibolite within the lowermost oceanic crust of the Limousin ophiolite. The role of

*Chargé de recherches du F.R.S.-FNRS.

†Aspirante du F.R.S.-FNRS.

fluid and elemental inputs into the amphibolites in the formation of the peraluminous mineral assemblages is also evaluated using geochemistry and a μ - μ diagram.

GEOLOGICAL SETTING OF THE LIMOUSIN OPHIOLITES AND OCCURRENCES OF CORUNDUM AMPHIBOLITES IN THE FMC

A nearly continuous unit of mafic-ultramafic bodies with oceanic affinities occurs as a tectonic unit in central Limousin (Dubuisson *et al.*, 1988, 1989) and it was recently mapped at the 1/10 000 scale (Fig. 2). These bodies lie above a major tectonic unit, the Lower Allochthon (also known as the Lower Gneiss Unit, LGU), mainly consisting of leucocratic fine-grained augen orthogneisses (locally known as 'leptynites'), which represent subalkaline and alkaline meta-granitoids dated by U-Pb geochronology on zircon: by ID-TIMS at 495 ± 8 Ma (Lafon, 1986) and by LA-ICP-MS on single grains at 475–464 Ma (Melleton *et al.*, 2009). Above the ophiolite massifs, the Upper Allochthon (also known as Upper Gneiss Unit, UGU) consists of plagioclasic paragneisses with many intercalations of eclogites, amphibolites and orthogneisses forming the so-called 'leptyno-amphibolite complex'. The protolith of the orthogneisses in this unit has been dated at *c.* 525 Ma in southern Limousin (Alexandrov *et al.*, 2001), but younger zircon has been analysed in the same area (470 Ma, Melleton *et al.*, 2009). Eclogites from the Upper Allochthon have not been dated in the Limousin but, following geochronological investigations in the whole Massif Central, the HP event is bracketed between 430 and 390 Ma (see Bellot & Roig, 2007, for a recent review). Oceanic relics are also undated in the FMC but following the review of Pin (1990), two periods of rifting and oceanization characterize the pre-suturing evolution of the European Variscan belt: a first one during Cambro-Ordovician times and a second stage probably during Devonian.

Corundum amphibolites, consisting of pargasite-anorthite associations with minor or accessory sapphirine, kyanite, gedrite and spinel, are widespread in the FMC (Fig. 1). They are present in the Haut-Allier (Forestier & Lasnier, 1969; Marchand *et al.*, 1989); in southern FMC (Aveyron; Messenier *et al.*, 1984), in Limousin (Piboule & Ménot, 1976; Ménot & Piboule, 1977; Floc'h *et al.*, 1979; Briand *et al.*, 1982; Santallier, 1994 and references therein; this study) and in Morvan (Godard, 1990). Despite the scatter of the various outcrops at the FMC scale, some common important geological characteristics are shared by all the occurrences: (i) they are found at the tectonic suture between the two main tectonic units of the FMC (Fig. 1), namely the LGU and UGU (Lower and Upper Allochthon); (ii) they belong to a thin tectonic unit composed of kyanite-garnet micaschists containing lenses of high grade basic/ultramafic rocks, i.e. garnet peridotites, granulites and eclogites (Floc'h *et al.*, 1979; Lasnier & Marchand, 1979; Messenier *et al.*, 1984);

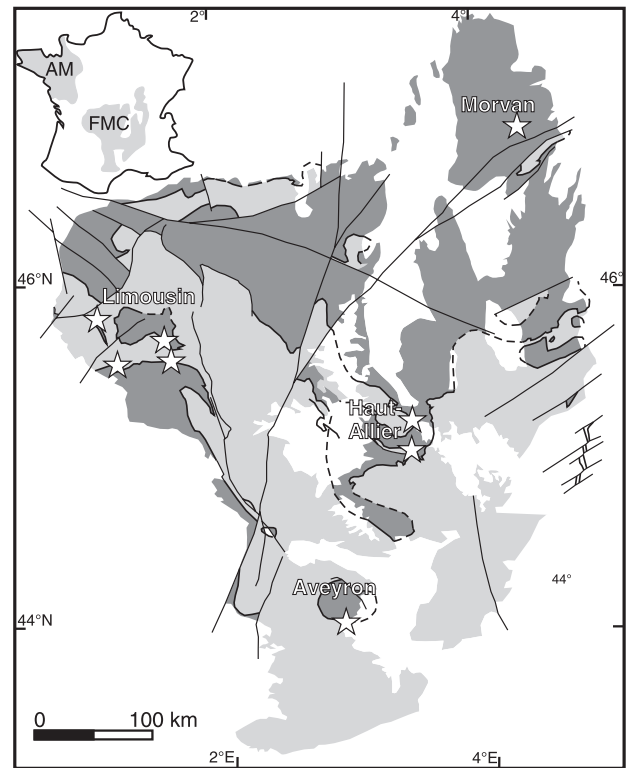


Fig. 1. Simplified map of the lithotectonic units of the French Massif Central. The light grey units represent the para-autochthon and the Lower Allochthon (Lower-Gneiss unit), the dark grey encompasses the Upper Allochthon (Upper-Gneiss unit) and the epizonal Thiviers-Payzac unit. The stars show the location of corundum-bearing amphibolite outcrops. The inset in the upper left corner shows the position of the Armorican massif and the French Massif Central (grey areas) in France.

(iii) they are also in close association with basic-ultramafic rocks devoid of high-grade recrystallization (flaser-gabbros and spinel-serpentinite outcropping nearby; Ménot & Piboule, 1977; Lasnier & Marchand, 1979; Santallier, 1994; this study). In Morvan, there is also evidence for a limited oceanization with the development of an ensialic marginal basin as attested by pillow lavas, and gabbros with both mid-ocean ridge (MOR) and supra-subduction zone (SSZ) fingerprints (Sider & Ohnenstetter, 1986; Ohnenstetter, 1994).

In central Limousin (this study), the relationships between the corundum-bearing amphibolites and the ophiolitic massifs are well exposed. The results of the new mapping campaign demonstrate that the ophiolitic bodies are underlain by a thin but nearly continuous micaschist unit with some intercalations of leucocratic orthogneisses and both zoisite- and kyanite-eclogites at its base. Micaschists rarely crop out in central Limousin but on the basis of the description of Chenevoy *et al.* (1990), they are similar to the kyanite-micaschist associated with corundum-bearing amphibolites in the FMC as a whole. Both micaschists and ophiolitic bodies have been grouped

into the same tectonic unit called the Middle Allochthon (Dubuisson *et al.*, 1988) corresponding to the Middle Allochthon defined by Ballèvre *et al.* (2009) in the Southern Armorican massif. The Limousin ophiolite comprises a mantle section dominated by serpentinized Cpx-bearing spinel harzburgite topped by small layers of dunites with podiform chromitites in most of the massifs. The base of the crustal section consists of layered olivine-bearing cumulates (mainly spinel-troctolites with wehrlites) and is overlain by oxide-free faser-gabbros and amphibolites, whereas Fe–Ti gabbros/amphibolites dominate the upper parts of the crustal section. Other lithologies typical of oceanic rocks have been found as dykes intruding the gabbros: plagiogranites (quartz + albite), prehnite-bearing epidotes, rodingites (metasomatized gabbros with hydrogarnet, prehnite and epidote) and fine-grained amphibolitized Fe–Ti gabbros. Most of the lithologies were affected by ocean-floor metamorphism (Berger *et al.*, 2005) with no evidence for MP or HP recrystallization, except for the presence of a few corundum–kyanite–sapphirine–gedrite amphibolites discussed in this study. These rocks crop out at the boundary zone between troctolites and gabbros; they are closely associated with serpentinized, olivine-rich troctolites characterized by the presence of coarse (up to 2 cm wide) blue–green and brown spinel. Most of the corundum-bearing amphibolites are more deformed than the surrounding troctolites, as in western Limousin where they are affected by recumbent folds synchronous of garnet poikiloblast growth (Floc'h *et al.*, 1979). Pargasite shows a well-defined shape preferred orientation and plagioclase underwent grain-size reduction due to incomplete dynamic recrystallization.

The ophiolitic massifs form overturned anticlines, with axial plane moderately to steeply dipping to the N–NE (Fig. 2). Some rare shear-sense indicators indicate a top-to-the-W/SW movement of the ophiolitic bodies.

PETROGRAPHIC NOTES AND MINERAL CHEMISTRY

The different rocks sampled for this study form a coherent sequence from magmatic troctolites to completely recrystallized kyanite–sapphirine–gedrite amphibolites (Table 1). One specific sample (L04-57) is heterogeneous and shows both the preserved magmatic associations and the development of pargasite and corundum within a 3-cm-thick vein and the surrounding reaction zone. Gabbros and hydrothermal rocks are described in detail in two companion papers (Berger *et al.*, 2005, 2006).

The mineral compositions were measured using a CAMECA SX100 electron microprobe at the University Henri Poincaré at Nancy (France). Counting times for peak and background intensity were fixed at 10 s. Calibration was carried through with a set of

artificial and natural crystal standards. Data reductions were obtained by application of the PAP program (Pouchou & Pichoir, 1991).

Troctolites

They are medium-grained rocks consisting of rounded and partly serpentinized olivine with polygonal grains of plagioclase. Minor phases are brown chromian spinel and minor clinopyroxene. All the intermediate compositions between plagioclase-dunite and olivine-bearing anorthosite are found. Plagioclase is intermediate to calcic (An_{60-80}), olivine has a restricted range of composition (Fo_{80-87}) and spinel has a wide range of Cr content ($Chr_{12-55}Mg_{0-16}Spl_{18-71}Hc_{6-21}$) controlling the Fe^{2+} Cr \leftrightarrow MgAl reciprocal substitution (Table 2) but very low Ti (below detection limits except in sample L04-77 where the proportion of the ulvöspinel component reaches 1 mol.%). Accessory magmatic phases are clinopyroxene (Mg#: 88–91) and rare orthopyroxene (Mg#: 85–86). The post-magmatic transformations include the pervasive serpentinization of olivine and the transformation of plagioclase into a chlorite + prehnite assemblage. These modifications have been attributed to ocean-floor hydrothermal metamorphism (Berger *et al.*, 2005).

Anhydrous coronitic troctolites

The mineral associations, compositions and textures of this rock type are the same as those observed in troctolites *s. str.*, but a thin reactional corona is present between the olivine and plagioclase grains (Fig. 3a). At the first stage of the metamorphic exchange, the corona consists of clinopyroxene, orthopyroxene and spinel. This reaction can be written as follows:



The newly formed pyroxene (Table 3) has lower Al contents and lower Mg#'s (opx: 83–84; cpx: 83–95) and the coronitic spinel is totally devoid of Cr and Fe^{3+} ($Spl_{71}Hc_{29}$).

Hydrous coronitic troctolites

In such troctolites, fibrous to nematoblastic pargasite is observed in the olivine–plagioclase coronæ and may totally replace the former two-pyroxene–spinel associations. The amphibole (Table 4) is now strongly enriched in Al (up to 20 Al_2O_3 wt%) and Mg (Mg#: 83–93). In some samples, pargasite grows at the expense of olivine and some thin sections show aggregates of polygonal pargasite completely invading the former textural sites of olivine. The brown chromian spinel partly transforms into blue–green spinel totally devoid of Cr ($Spl_{68-76}Hc_{24-32}$; Fig. 5b, Table 6), the released Cr being incorporated to the surrounding pargasite (up to 1.61 Cr_2O_3 wt%).

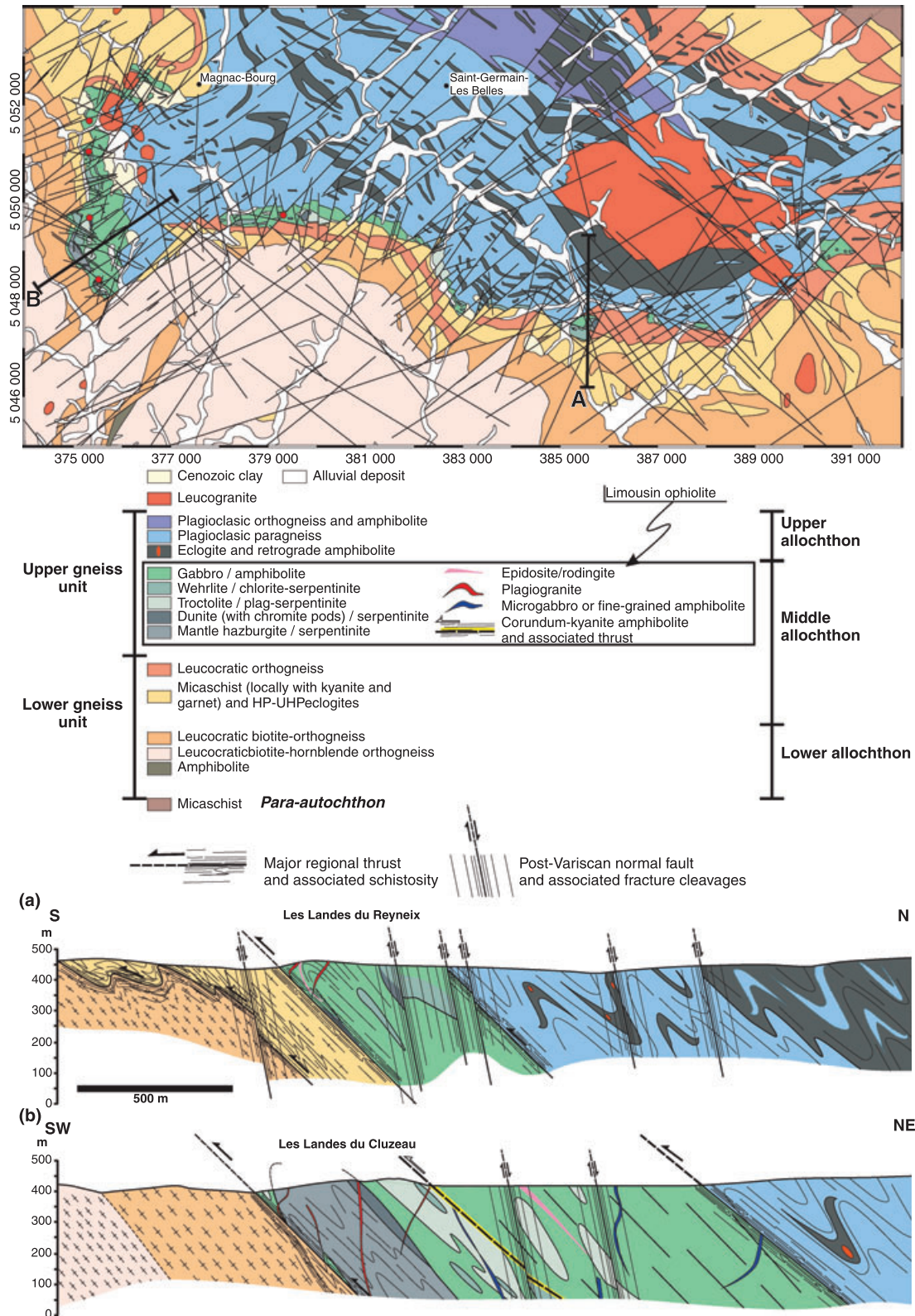


Fig. 2. Revised geological map and new cross-sections for Central Limousin (UTM coordinates, zone 31T, WGS 84 reference system). Lower/Upper Gneiss unit subdivision according to Faure *et al.* (2009); Lower/Middle/Upper Allochthon terminology from Dubuisson *et al.* (1988). Red dots show the locations of the corundum amphibolite samples and related rocks. Labels (a) and (b) refer to the location of cross sections in the map (heavy lines labeled A and B).

Table 1. Mineral associations in the main rock types.

	Coronitic troctolites									Serps with blue spl		Crn–ky–spr amphibolites			
	Limo 3	Limo 8	Limo 19	Limo 28	L04-57	L04-77	L04-92	L04-96	L04-132	L04-72	L04-135	L04-30	L04-40	L04-58	L04-102
Ol	+++	+++	+++	+++	+++	+++	+++	+++	+++	++	++				
Cpx	+			+			+		+						
Opx	+			+			+		+						
Cr–Spl	+	+	+	+	+	+	+	+	+				+		
Pl	+++	+++	+++	+++	+++	+++	+++	+++	+++						
Cpx	+	+					+	+							
Opx	+		+			+		+							
Al–Spl	+	+	+	+	+	+	+	+	+						
Amp	+		+	+	+	+	+	+	+	++	++	+++	+++	+++	+++
An												+++	+++	+++	
Al–Spl					+					++	++	+	+		
Cor					+							+	+		++
Ky												+	+	+	+
Spr												+	+	+	
Ged												+	+	+	
Mrg															+
Dia															+
Ms															+
Srp	+	+	+	+	+	+	+	+	+	++	++				
Chl										+	+				++
Ab												+	+	+	

+++ , abundant; ++ , minor; + , accessory.

Table 2. Representative compositions of the main magmatic minerals from the plutonic section of the Limousin ophiolite.

Sample Minerals	L04-132 Cpx	L04-132 Cpx	Limo 28 Cpx	L04-78 Cpx	L04-92 Opx	L04-132 Olivine	L04-92 Olivine	Limo 19 Olivine	L04-77 Spinel	L04-132 Spinel	L04-92 Spinel	L04-92 Plag	L04-57 Plag
Rock-type	Troctolite	Troctolite	Gabbro	Gabbro	Troctolite	Troctolite	Troctolite	Troctolite	Troctolite	Troctolite	Troctolite	Troctolite	Troctolite
SiO ₂	51.18	51.73	51.39	50.81	54.16	39.72	39.25	39.07				49.818	48.84
TiO ₂	1.22	0.93	0.61	0.87	0.15				0.55	0.00	0.02		
Al ₂ O ₃	4.00	3.58	3.58	3.44	3.38				14.12	41.51	53.00	30.741	32.17
Cr ₂ O ₃	0.75	0.69	0.20	0.63	0.19				44.27	22.70	11.31		
FeO	3.28	3.34	5.11	4.67	9.35	14.04	14.47	18.14	33.34	21.78	17.54	0.03	0.08
MnO	0.09	0.05	0.17	0.16	0.24	0.17	0.24	0.29	0.51	0.20	0.23		
MgO	15.31	15.43	14.35	15.31	31.08	45.35	45.27	42.41	4.03	11.56	15.89		
CaO	22.99	23.38	23.37	22.45	0.48	0.06	0.02	0.01				14.333	15.54
Na ₂ O	0.68	0.65	0.58	0.61								3.416	2.66
Sum	99.50	99.79	99.34	98.94	99.03	99.34	99.24	99.92	96.82	97.75	97.99	98.34	99.28
Mg#	91.2	91.5	86.1	89.4	85.4	85.2	84.8	80.6	20.9	50.8	64.8		
Al#									29.3	71.6	85.3		
Cr#									61.6	26.3	12.2		
An%												69.8	76.2

Mg#, $100 \times \text{Mg}/(\text{Mg} + \text{Fe}^{2+})$; Al#, $100 \times \text{Al}/(\text{Al} + \text{Cr} + \text{Fe}^{3+})$; Cr#, $100 \times \text{Cr}/(\text{Al} + \text{Cr} + \text{Fe}^{3+})$; An%, $100 \times \text{Ca}/(\text{Ca} + \text{Na} + \text{K})$.

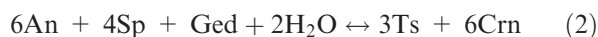
Mixed troctolite/corundum–pargasite sample

The coronitic troctolite L04-57 is cut by a 0.5-cm-thick vein consisting of fine-grained nematoblastic pargasite, spinel ($\text{Spl}_{68}\text{Hc}_{32}$), corundum and accessory plagioclase (Fig. 4) surrounded by a 2-cm-thick reaction zone where olivine and plagioclase are replaced by fibrous pargasite and nearly pure polygonal anorthite. Some olivine is completely transformed into pargasite.

Corundum-bearing amphibolites

They are composed of nematoblastic high-Al amphibole (pargasite/tschermakite, Mg#: 80–98; Fig. 5c, Table 4) in association with partly recrystallized small polygonal grains of nearly pure anorthite (An_{86-97} ; Fig. 5a, Table 5). Similar compositions are found in

the corundum-bearing metatroctolites of the Buck-Creek Variscan ophiolitic complex in the Appalachian belt (Tenthorey *et al.*, 1996; Peterson *et al.*, 2009). Corundum, surrounded by Cr–amphibole or within plagioclase patches, is either present as reddish ruby (Cr_2O_3 : 1.9 wt%) with numerous inclusions of brown spinel (Figs 3c & 5b, Tables 4 & 6; $\text{Chr}_{53-65}\text{Spl}_{35-47}$) or as rare small colourless grains with rare inclusions of Cr-free spinel (Cr below detection limit). These observations, together with the fact that gedrite is generally present close to corundum (Fig. 3f); suggest that corundum was formed according to the following reaction in the CMASH system:



Corundum is generally small ($\sim 200 \mu\text{m}$), but some of the colourless grains reach 1 cm in diameter.

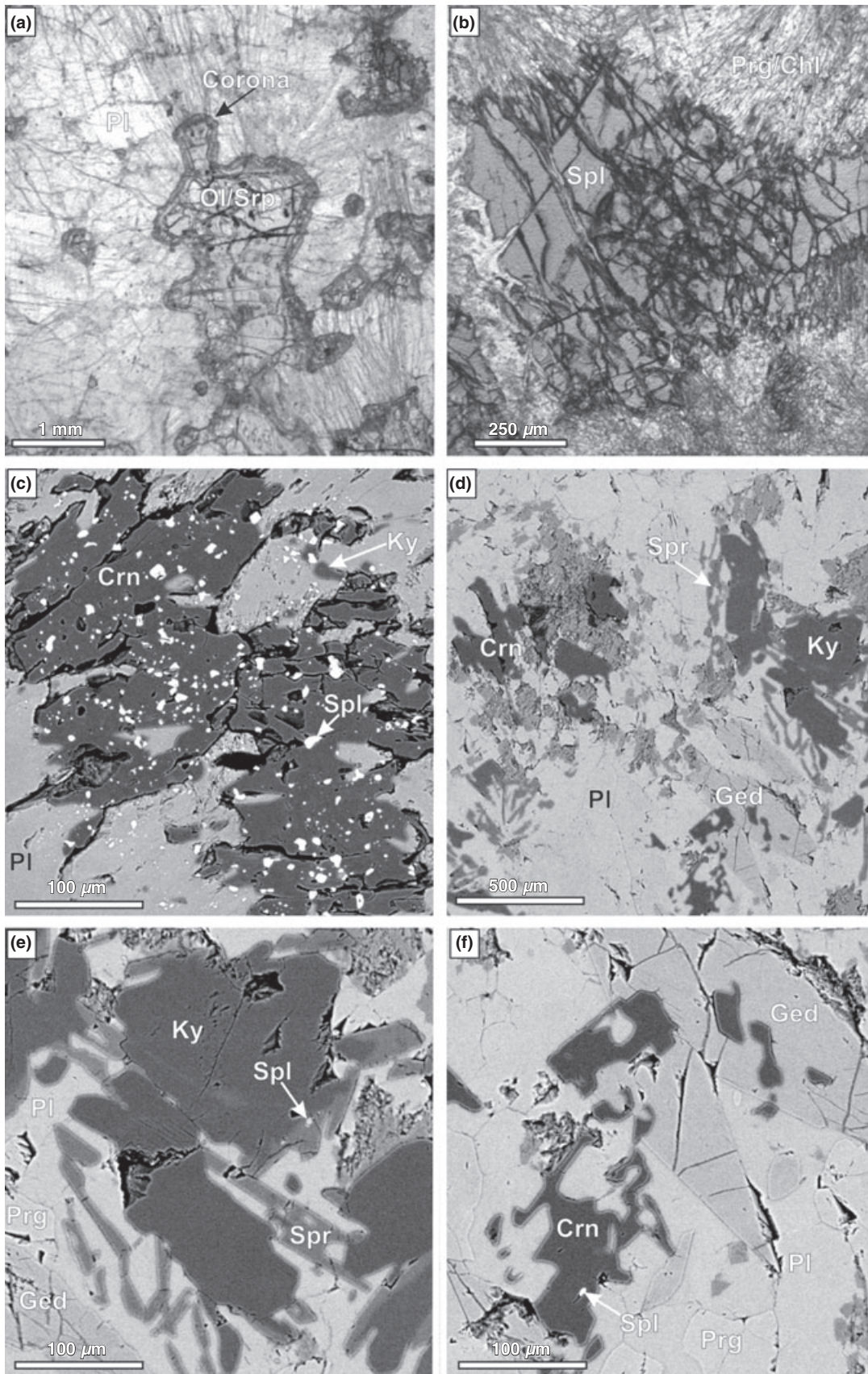
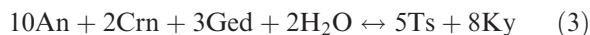


Table 3. Composition of the secondary coronitic pyroxene.

Sample Name	Limo 3 Cpx	L04-96 Cpx	Limo 3 Opx	L04-96 Opx
Type	Ol-Pl cor	Ol-Pl cor	Ol-Pl cor	Ol-Pl cor
SiO ₂	52.23	52.41	56.11	57.62
TiO ₂	0.47	0.32		
Al ₂ O ₃	2.99	3.66	2.28	0.88
Cr ₂ O ₃	0.24	0.31		
FeO	5.54	2.71	10.55	10.18
MnO	0.27	0.10	0.17	0.22
MgO	14.64	15.95	31.37	32.24
CaO	22.46	23.20	0.15	0.11
Na ₂ O	0.51	0.72		
Sum	99.35	99.38	100.63	101.24
Si	1.93	1.92	1.96	1.99
Ti	0.01	0.01		
Al	0.13	0.16	0.09	0.04
Cr	0.01	0.01		
Fe ³⁺	0.01	0.04		
Fe ²⁺	0.17	0.04	0.31	0.29
Mn	0.01	0.00	0.01	0.01
Mg	0.81	0.87	1.63	1.66
Ca	0.89	0.91	0.01	0.01
Na	0.04	0.05		
Sum	4.00	4.01	4.00	4.00
Mg#	83.0	95.4	84.1	85.0

In most samples, corundum is partly to totally replaced by small elongated grains of kyanite (Fig. 3c). However, the kyanite-forming reaction cannot be

determined on a petrographical basis because no clear reactional texture was observed. As clino- and ortho-amphibole are present in the vicinity of corundum–kyanite assemblages, the following reaction is proposed in the CMASH system:



Sapphirine crystallization most probably results from reaction between kyanite and spinel, because small spinel inclusions are still frequently present at the contact zone between kyanite and sapphirine (Fig. 3e). Again, no clear reactional textures have been observed but the following reaction can be proposed in the MASH system:



As for its composition (Table 6), the Mg–sapphirine (Mg#: 89–91) from Limousin lies out between the 7:9:3 and 3:5:1 MAS species (Fig. 5d), and it is among the most peraluminous sapphirine found yet in metabasites.

Long (up to 3 cm long) acicular gedrite (Mg#: 81–83) is observed in the corundum amphibolites. Corundum is either found as inclusions in the gedrite crystals or grows at its borders (Fig. 3f). Gedrite is

Table 4. Representative compositions of clino- and ortho-amphibole.

Sample Name	L04-57 Parg	L04-57 Parg	L04-40 Parg	L04-58 Tscherm	L04-102 Parg	L04-40 Parg	L04-37 Tscherm	L04-30 Mg-Hornb	L04-58 Mg-Hornb	L04-37 Mg-Hornb	L04-30 Gedrite	L04-40 Gedrite
Type	Ol-Pl cor	Vein	Matrix	Matrix	Matrix	Matrix	Matrix	Matrix	Secondary	Secondary	Matrix	Matrix
SiO ₂	43.24	41.58	43.96	44.99	45.18	44.67	43.67	47.23	49.72	49.72	45.11	43.42
TiO ₂			0.10	0.19	0.07	0.23	1.14		0.18	0.28	0.11	
Al ₂ O ₃	16.85	18.41	17.38	16.97	16.18	16.17	14.70	14.33	9.67	6.91	18.92	20.75
Cr ₂ O ₃	0.07	0.00	1.61	0.08		1.81	0.65	0.09	0.60	0.10	0.11	0.18
FeO	5.13	7.58	5.33	5.77	7.08	5.27	5.96	5.15	5.17	4.84	8.46	8.45
MnO	0.08	0.05	0.15	0.12		0.15	0.03	0.03	0.12	0.11	0.13	0.23
MgO	16.05	14.01	15.14	15.66	15.19	15.41	16.27	16.59	18.23	19.69	22.35	21.48
CaO	12.27	11.51	11.88	11.42	11.71	11.52	12.08	12.02	11.73	12.10	0.58	0.55
Na ₂ O	2.76	2.82	2.20	2.10	2.10	2.13	2.56	1.59	1.18	1.51	1.88	2.39
K ₂ O	0.13	0.04	0.12	0.08	0.05	0.06	0.13	0.05	0.04			
Sum	96.60	96.00	97.85	97.39	97.55	97.26	97.30	97.08	96.63	95.25	97.64	97.50
Si	6.17	6.01	6.18	6.30	6.36	6.30	6.22	6.61	6.98	7.09	6.16	5.97
Ti			0.01	0.02	0.01	0.02	0.12		0.02	0.03	0.01	
Al	2.83	3.14	2.88	2.80	2.69	2.69	2.47	2.37	1.60	1.16	3.04	3.36
Cr	0.01	0.00	0.18	0.01		0.20	0.07	0.01	0.07	0.01	0.01	0.02
Fe ³⁺	0.17	0.31	0.23	0.34	0.29	0.25	0.23	0.22	0.30	0.33	0.43	0.36
Fe ²⁺	0.44	0.61	0.40	0.34	0.54	0.37	0.48	0.38	0.31	0.25	0.54	0.61
Mn	0.01	0.01	0.02	0.01		0.02	0.02	0.00	0.01	0.01	0.01	0.03
Mg	3.41	3.02	3.17	3.27	3.19	3.24	3.46	3.46	3.81	4.19	4.55	4.40
Ca	1.88	1.78	1.79	1.71	1.77	1.74	1.84	1.80	1.76	1.85	0.08	0.08
Na	0.76	0.79	0.60	0.57	0.57	0.58	0.71	0.43	0.32	0.42	0.50	0.64
K	0.02	0.01	0.02	0.01	0.01	0.01	0.02	0.01	0.01			
Sum	15.71	15.67	15.48	15.40	15.43	15.41	15.64	15.31	15.19	15.34	15.34	15.47
Mg#	88.6	83.2	88.9	90.6	85.5	89.8	87.8	90.0	92.6	94.4	89.5	87.8

Fig. 3. Photomicrographs of corundum-bearing amphibolites and related rocks: (a) anhydrous coronitic troctolites showing the development of a two-pyroxene reaction rim between olivine and plagioclase (transmitted light, Limo 3); (b) coarse blue–green spinel in an olivine-rich plagioclase–serpentine (transmitted light, L04-133); (c) reddish corundum containing chromian spinel inclusions in a pargasite-dominant matrix (BSE image; note the small kyanite grains at the border of corundum; L04-40); (d) kyanite–sapphirine associations in a polygonal plagioclase patch illustrating the breakdown products of corundum-bearing assemblages in a pargasite–anorthite amphibolite (BSE image; L04-30); (e) coarse kyanite grains with overgrowths of sapphirine in the presence of relict spinel grains (BSE image; L04-30); (f) corundum–gedrite association in a pargasite–anorthite amphibolite (BSE image; L04-30).

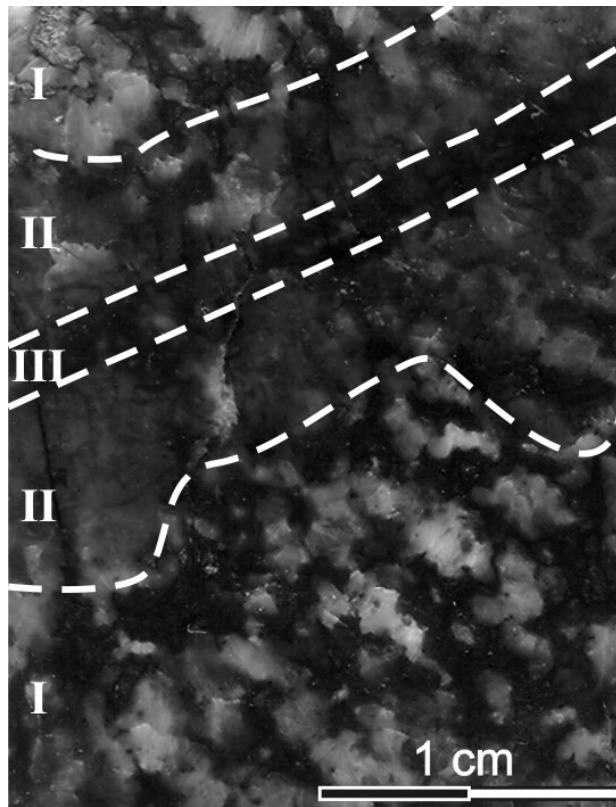


Fig. 4. Photograph of sample L04-57 showing both the preserved troctolite mineralogy and a vein consisting of pargasite, spinel and corundum. Pargasite progressively replaces olivine through a thin reaction zone on each side of the vein. I: coronitic troctolite (unmodified host); II: pargasite-bearing metatroctolite (reaction zone); III: pargasite–corundum ± spinel ± anorthite vein.

usually present in kyanite–sapphirine microdomains, which justifies it as a reactant of kyanite- and sapphirine-forming reactions. This orthoamphibole is unusually rich in Na (1.8–2.4 Na₂O wt%) and Al (from 15 to 21 Al₂O₃ wt%, Table 4). Similar Na–gedrite is found in a deep-seated olivine–gabbros (Otten, 1984) where it coexists with hornblende in coronae forming at olivine–plagioclase interfaces.

Several hydrous minerals indicate a retrogression of the previous assemblages. Margarite (Table 7) is frequently observed around corundum, together with Mg–chlorite, muscovite (Table 7) and rare diaspore (Table 6). The pargasite–anorthite assemblage is locally replaced by lower temperature pairs (Tables 4 & 5), i.e. Mg–hornblende (Si: 6.3–7.4 p.f.u.; Mg#: 87–95) and intermediate plagioclase (An_{35–55}). On the other hand, gedrite is frequently transformed into albite–chlorite fine-grained intergrowths.

Serpentinite with blue spinel

In former olivine-rich troctolites, consisting of < 10 vol.% of plagioclase, the brown chrome-spinel transforms into coarse anhedral blue spinel (Spl₆₈Hc₃₂; up

to 1 cm in size). This spinel is always surrounded by fibrous pargasite, which also completely replaces epigenetically all the former plagioclase.

Chlorite–pargasites

These samples have been previously described by Berger *et al.* (2005) as resulting from hydrothermal alteration of gabbros. In this study, these rocks are interpreted as former pargasite–gedrite rocks that underwent retrogression at amphibolite and greenschist facies conditions. Pargasite is the dominant phase, forming at least 60 vol.% of the rocks, with plagioclase as the second major constituent. An acicular phase now replaced by a chlorite–albite ± prehnite association is interpreted as representing former gedrite grains, by analogy to what is observed in corundum amphibolites. The texture of pargasite is variable, with polygonal aggregates that evolves progressively towards associations of nematoblastic to fibrous grains. Pargasite is Al- and Na-rich (13–17 wt% Al₂O₃; 2.0–3.3 wt% Na₂O) and shows a high Mg# (80–90). This amphibole is locally replaced by chlorite–Mg–hornblende associations.

ESTIMATION OF *P–T* CONDITIONS

The thermodynamic calculations were performed with THERMOCALC 3.33 (Powell & Holland, 1988) and data set 5.5 (Holland & Powell, 1998; November 2003 upgrade), with the an ordered activity–composition model for feldspar, a two-site mixing model for spinel and olivine (see Holland & Powell, 1998) and the activity model of Will & Powell (1992) for amphibole. The more recent solution model of Dale *et al.* (2005) has been tested but it gives too low a tschermakite activity (0.01–0.03) and a high tremolite activity (~0.7) when applied to the amphibole associated with corundum and kyanite. The tschermakite activity values (0.20–0.35) computed with the model presented by Will & Powell (1992) are more consistent with our amphibole composition and the thermodynamic calculations using these values yield *P–T* conditions comparable to those determined with the thermometer of Holland & Blundy (1994). Gedrite, kyanite, sapphirine (7:9:3 species) and corundum were taken as end-members. Various transfer and exchange thermometers (see references below) were also used in combination with thermodynamic modelling of reactions (1–3).

Petrogenetic grid in the CMASH system

To decipher the *P–T* evolution of the corundum amphibolite, a petrogenetic grid was drawn by using THERMOCALC 3.33 and Schreinemaker's analysis; only the stable intersections are presented on Fig. 6. Because the corundum amphibolites are largely dominated by the CaO–MgO–Al₂O₃–SiO₂–H₂O components (~95% of the whole-rock composition),

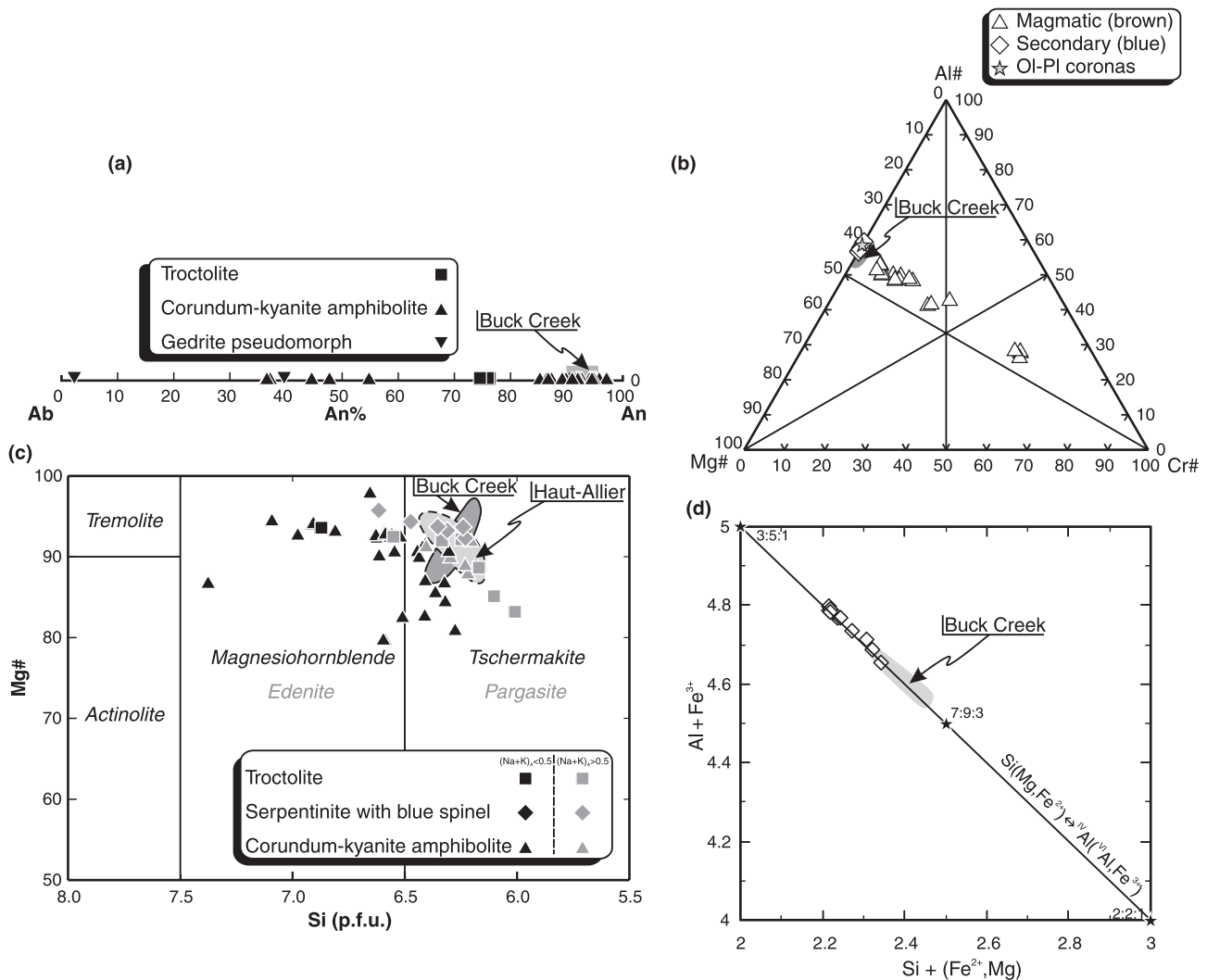


Fig. 5. Composition of the main minerals from the corundum-bearing amphibolites and related rocks: (a) plagioclase composition on the An–Ab join; (b) compositions of magmatic brown and secondary blue–green spinels; (c) amphibole compositions in Leake *et al.* (1997) classification diagram; (d) compositions of sapphirine. Reference compositional fields: Buck-Creek Variscan ophiolitic complex (Tenthorey *et al.*, 1996) and Haut-Allier corundum-bearing amphibolites (Forestier & Lasnier, 1969).

the CMASH system was chosen for simplicity. The phases used were tschermakite, anorthite (both in excess), gedrite, spinel, corundum, kyanite, sapphirine 7:9:3 and water. No quartz has been involved in the calculation because the amphibolites are Si-undersaturated rocks (44–45 wt% SiO₂). Thin-section analysis shows that the mineral associations have evolved from pargasite–anorthite–spinel rocks to pargasite–anorthite–corundum ± spinel ± gedrite to pargasite–anorthite–kyanite–sapphirine ± spinel ± gedrite assemblages. The *P–T* grid of Fig. 6 clearly demonstrates that reactions (2) and (3) have to be crossed over in the course of a pressure increase and/or a temperature decrease. Because thermobarometry shows that temperature is constant during evolution of coronitic troctolites into corundum–kyanite–sapphirine amphibolites (see below) this evolution in mineral association can be related to a temporal pressure

increase (from ~6 to 10 kbar) without significant modification of temperature (700–800 °C). The first sapphirine forming reaction



to be crossed over by the *P–T* path on Fig. 6 does not involve consumption of kyanite and thus, is not in agreement with petrographical observations. The proposed sapphirine-forming reaction (4) is not present in the CMASH diagram because it involves five phases instead of six for an univariant reaction in the CMASH system. In the MASH subsystem, reaction (4) has a positive slope in the *P–T* grid, but it is crossed over in the sense of sapphirine-consuming reaction following the proposed *P–T* path. As this is inconsistent with the main path established from CMASH modelling and thermobarometry, the possible influence of local compositional changes due to the existence of

Table 5. Representative compositions of metamorphic plagioclase.

Sample Type	L04-30a Matrix	L04-30b Matrix	L04-40a Matrix	L04-40b Matrix	L04-58a Matrix	L04-58 Matrix	L04-102a Secondary	L04-58 Secondary	L04-58 Gedrite
SiO ₂	43.27	45.72	44.19	44.42	44.19	46.18	59.51	58.29	67.03
Al ₂ O ₃	36.64	34.66	36.10	34.96	35.45	33.81	26.15	25.89	19.46
FeO					0.15	0.08	0.11	0.39	0.54
CaO	19.71	18.33	19.42	18.91	19.18	18.00	7.55	8.21	0.40
Na ₂ O	0.30	1.14	0.46	0.88	0.57	1.44	7.22	6.92	11.02
K ₂ O							0.07	0.14	0.10
Sum	99.92	99.84	100.17	99.17	99.54	99.50	100.62	99.84	98.55
Si	2.00	2.11	2.04	2.07	2.05	2.14	2.64	2.62	2.98
Al	2.00	1.88	1.96	1.92	1.94	1.84	1.37	1.37	1.02
Fe					0.01	0.01	0.01	0.01	0.02
Ca	0.98	0.91	0.96	0.94	0.95	0.89	0.36	0.39	0.02
Na	0.03	0.10	0.04	0.08	0.05	0.13	0.62	0.60	0.95
K							0.01	0.01	0.01
Sum	5.01	5.00	5.00	5.01	5.00	5.01	5.00	5.00	4.99
An%	97.3	89.9	95.9	92.2	94.9	87.4	36.5	39.3	2.0
Ab%	2.7	10.1	4.1	7.8	5.1	12.6	63.1	59.9	97.4
Or%							0.4	0.8	0.6

chemical gradients within samples or metasomatism is explored in the discussion section.

Thermobarometry

Magmatic crystallization has been qualitatively estimated (Berger *et al.*, 2005, 2006) to have occurred under relatively low pressures as pyroxene has compositions comparable to those for oceanic gabbros rather than to high-Al pyroxene of deep-seated intrusions and granulites. Using the temperature-independent structural barometer of Nimis & Ulmer (1998), the pressure estimated from clinopyroxene isolated from orthopyroxene and without exsolutions, ranges between 0.5 ± 1.7 and 2.6 ± 1.7 kbar for troctolites and gabbros. This is in agreement with experiments showing that olivine and plagioclase (phases coexisting in troctolites and olivine-gabbros) crystallize together at low to moderate pressures in tholeiitic basalts (Villiger *et al.*, 2004).

The P – T conditions for coronæ growth between olivine and plagioclase can be estimated through two-pyroxene thermometry (Bertrand & Mercier, 1985) as well as thermodynamic modelling of reaction (1) by using THERMOCALC (Holland & Powell, 1998) as well as TWQ softwares (Berman, 1988). The intersection of the curves yields values of $\sim 780 \pm 18$ °C at 7.0 ± 1.3 kbar for samples Limo-3 and L04-96. (Fig. 7a), whereas multiequilibrium thermobarometry yields a unique solution at 800 °C and 6 kbar (Fig. 7b) with TWQ for the formation of coronæ in sample Limo-3.

The condition for corundum formation can be estimated using thermodynamic modelling of reaction (2) and the amphibole-plagioclase thermometer of Holland & Blundy (1994). Using THERMOCALC, reaction (2) has been calibrated for samples L04-30 and L04-40 (Fig. 8), and the intersection of this reaction with the results from amphibole-plagioclase thermometry yields P – T conditions in the range of 800 – 820 ± 36 °C and

9.1 – 10.5 ± 1.0 kbar [errors presented here are the uncertainties on P – T calibration of reaction (2) using THERMOCALC]. The same approach has been used for the kyanite-in reaction (3) and the computed P – T conditions are within the error range of those for corundum formation: 820 – 830 ± 54 °C and 10.1 – 10.8 ± 1.4 kbar.

The P – T conditions for sapphirine-forming reactions cannot be precisely determined, mostly due to the poorly known thermodynamic properties and activity composition relationships of sapphirine (for a recent review, see Podlesskii *et al.*, 2008). However, amphibole-plagioclase pairs in close association with sapphirine gives temperatures of equilibration between 810 and 830 °C for sample L04-30; 820 and 830 °C for sample L04-40, and 810 and 830 °C for sample L04-58 (pressure fixed at 10 kbar, error of ± 40 °C, as proposed by Holland & Blundy, 1994). The sapphirine-spinel Fe–Mg exchange thermometer of Sato *et al.* (2006) also yields temperatures quite similar, bracketed between 780 and 830 °C for pressure fixed at 10 kbar, which is well in the range of the kyanite-sapphirine stability field (Fig. 11) determined by Podlesskii *et al.* (2008).

Mg-hornblende, intermediate plagioclase, chlorite, margarite and diaspore partly overprint the HT associations described above. The P – T conditions for Mg-hornblende to form can be estimated with the semi-quantitative Al-in-hornblende barometer of Schmidt (1992) and the exchange thermometer of Holland & Blundy (1994). Results for samples L04-57 and 58 are bracketed between 630 – 670 ± 40 °C and 6 ± 2 kbar. As for the chlorite–albite assemblage replacing gedrite, it clearly suggests a moderate recrystallization in greenschist facies conditions below 550 °C (Spear, 1993).

GEOCHEMISTRY

The analyses were carried out at the ‘Service d’Analyse des Roches et des Minéraux’ (SARM at the CRPG,

Table 6. Representative compositions of corundum, diaspore, spinel, kyanite and sapphirine in the Limousin samples.

Sample Name	L04-30 Corundum Matrix	L04-40 Corundum Matrix	L04-40 Corundum Matrix	L04-57 Corundum Vein	L04-57 Ol-Pl Cor	L04-40 Spinel Incl Crn	L04-37 Spine Blue	L04-72 Spinel Blue	L04-72 Spinel Blue	L04-72 Spinel Blue	L04-135 Spinel Blue	L04-58 Spinel Incl Sap	L04-30 Kyanite Matrix	L04-40 Kyanite Matrix	L04-58 Kyanite Matrix	L04-30 Sapphirine Matrix	L04-40 Sapphirine Matrix	L04-58 Sapphirine Matrix
SiO ₂	99.37	97.37	99.49	99.27	66.44	40.78	60.79	66.06	66.28	66.06	65.94	64.45	37.13	36.75	36.85	11.52	11.06	11.04
Al ₂ O ₃		1.96				23.48	2.20	0.81	0.86	0.81	0.19		62.31	62.84	63.25	67.43	66.73	69.30
Cr ₂ O ₃	0.21	0.41	0.13	0.20	14.51	21.32	16.79	12.50	12.49	12.50	13.04	15.17		0.09	0.25	3.37	3.39	3.53
MnO					0.09	0.12	0.07	0.11	0.06	0.11								0.07
MgO					17.96	10.20	16.60	19.22	19.37	19.37	19.39	17.36						17.47
CaO																		
Sum	99.57	99.74	99.62	99.48	98.99	95.90	96.44	98.69	99.06	98.69	98.55	96.97	99.44	99.68	100.35	99.91	98.83	101.41
Si																		
Al	2.00	1.97	2.00	2.00	2.00	1.45	1.92	1.98	1.98	1.98	1.98	1.99	1.01	1.00	0.99	0.67	0.65	0.64
Cr		0.03				0.56	0.05	0.02	0.02	0.02	0.00		1.99	2.01	2.01	4.64	4.65	4.70
Fe ²⁺						0.32	0.34	0.27	0.27	0.26	0.02	0.32						0.14
Fe ³⁺	0.01	0.01	0.01	0.01	0.01	0.01	0.01	0.01	0.01	0.01	0.02	0.01		0.01	0.01	0.02	0.07	0.03
MnO						0.68	0.66	0.73	0.73	0.73	0.74	0.68						0.01
Mg																		1.50
Cu																		
Sum	2.01	2.00	2.01	2.01	3.01	3.01	3.01	3.01	3.01	3.01	3.00	3.00	3.00	3.01	3.00	7.01	7.02	7.02
Mg#																		
Al#																		
Cr#																		

Nancy). Major elements were analysed by ICP–OES and trace elements by ICP–MS according to the methods described in Carignan *et al.* (2001). Results are presented as supplementary electronic material.

Whole-rock compositions of the corundum–kyanite amphibolites are plotted in Fig. 9a,b together with the main rock types of the ophiolitic section and other pargasite-bearing rocks. The corundum-bearing amphibolites have globally the same composition as the plagioclase-rich troctolites (i.e. high content in Al and Ca, but low levels for Si) whereas the blue spinel–serpentinites are close to olivine-rich troctolite compositions. They lie exactly in the compositional field formed by olivine and plagioclase microprobe analyses in troctolites (Fig. 9b). Accordingly, these three groups of rocks show a strong positive Eu anomaly ($Eu/Eu^*: 1.25–5$) and LREE-depleted to LREE-enriched patterns [$(La/Yb)_N: 0.3–4.5$]. These patterns are similar to those for the troctolites and low-REE gabbros of the Limousin ophiolites (Fig. 9c,d). The high Al-content of corundum-bearing amphibolites (up to 27 wt% Al_2O_3) compared with that of other pargasite-bearing rocks (<25 wt%) probably controls the formation of peraluminous minerals (corundum, kyanite, sapphirine) during recrystallization under HT and MP conditions. Serpentinites with blue spinel are comparable to olivine-rich troctolites (higher mean MgO contents compared with corundum-bearing amphibolites) and were probably not sufficiently enriched in Al_2O_3 (and, accordingly, in former magmatic plagioclase) to crystallize corundum, kyanite and sapphirine during the peak $P–T$ conditions. Amphibolites L04-30/40 and troctolites Limo 3 and L04-132 have nearly exactly the same major element composition except for higher content in CaO and Al_2O_3 in amphibolites (12.6–13.3 and 25.6–25.7 wt% respectively) compared with troctolites (9.3–10.3 and 20.9–24.7 wt% respectively). The trace-element content of samples L04-30/40 and troctolite Limo 3 are also strikingly similar except for higher contents in Ba and Sr, i.e. elements generally substituted to Ca, in the corundum amphibolites.

Gabbros are characterized by lower Al contents (15–23 Al_2O_3 wt%) but higher Ca values when compared with troctolites, which reflects the presence of clinopyroxene (Fig. 9a). Their REE patterns also show a strong positive Eu anomaly, with both LREE-depleted and enriched patterns (Fig. 9c). Some Fe–Ti gabbros show a smooth REE pattern with some depletion in LREE [$(La/Yb)_N: 0.3–0.8$] and a high mean REE content (around 10 times the chondritic value), suggesting that they probably correspond to mafic chilled melts rather than cumulates. These three samples can be used to infer the presence of a recycled crustal component within their mantle source, which can help to discriminate the oceanic tectonic setting for the formation of the ophiolites. Their LREE-depleted patterns are common in basalts both from MOR environments (N-MORBs) and back-arc basins. Two

Table 7. Representative compositions of secondary hydrous phyllosilicates.

	L04-102 Margarite	L04-102 Margarite	L04-102 Muscovite	L04-102 Chlorite	L04-102 Chlorite	L04-58 Chlorite
SiO ₂	32.44	38.45	45.77	27.57	28.70	30.22
Al ₂ O ₃	48.07	45.08	37.08	23.62	22.96	18.98
FeO				10.38	9.99	9.27
MnO				0.08		0.17
MgO	0.05	0.08	0.28	26.31	26.42	26.88
CaO	11.27	6.79	0.19	0.05		
Na ₂ O	1.67	4.01	0.22			
K ₂ O	0.07	0.10	10.90			
Sum	93.56	94.51	94.43	88.00	88.08	85.52
Si	2.18	2.52	3.05	2.66	2.76	2.80
Al	3.81	3.48	2.91	2.69	2.60	2.53
Fe				0.84	0.80	0.79
Mn				0.01		0.01
Mg	0.01	0.01	0.03	3.79	3.78	3.80
Ca	0.81	0.48	0.01	0.01		
Na	0.22	0.51	0.03			
K	0.01	0.01	0.93			
Sum	7.03	7.00	6.96	9.99	9.94	9.92

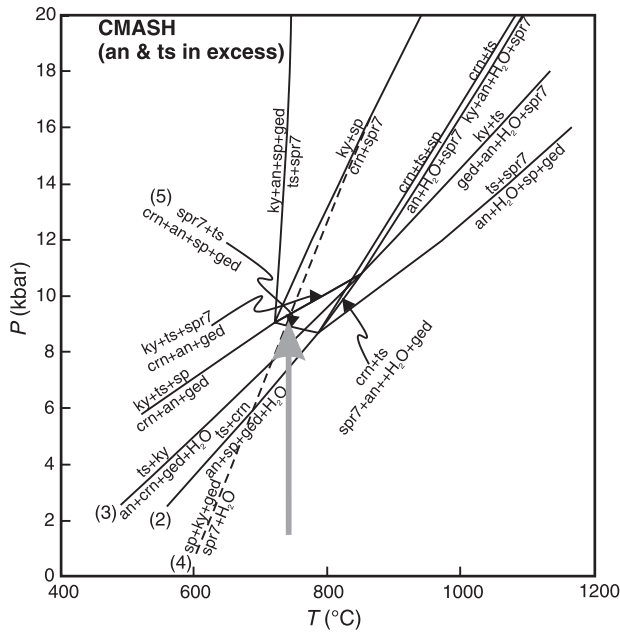


Fig. 6. P - T grid in the CMASH system calculated using THERMOCALC; tschermakite and anorthite are in excess. The sapphirine-forming and kyanite-consuming reaction (dashed line) in the MASH subsystem is also shown. Tschermakite and anorthite are in excess. Numbers beside some univariant curves refers to reactions quoted in the text. The grey arrow roughly shows the probable prograde P - T path according to P - T calculations results (see Figs 7 & 8).

samples show no significant Nb anomaly (Nb/Nb^* : 0.7–0.9) whereas most back-arc basalts show a strong negative Nb anomaly (from 0.2 to 0.8 with a mean at 0.6). N-MORBs from the Indian Ocean do not show a pronounced Nb anomaly (Nb/Nb^* : 0.6–1.3, mean: 0.95) and the immobile trace-element pattern of sample L04-83 is very similar to those of the most depleted

N-MORBs from the Indian Ocean (Fig. 10). However, one sample from the Limousin ophiolite has a strong negative Nb anomaly (Fig. 10), which clearly indicates that recycled crustal components were present in the mantle source. The combination of both MOR and SSZ geochemical fingerprints observed in the Limousin ophiolite is common in Tethyan and other worldwide ophiolites (Pearce, 2003; Dilek *et al.*, 2008) and probably reflects an evolution of the tectonic setting of formation.

DISCUSSION

Metamorphic evolution and tectonic significance of the corundum-bearing amphibolites

The crystallization pressure of the troctolites is low, below 2 kbar, in agreement with the conditions of oceanic crust formation. This work demonstrates that some plagioclase-rich troctolites belonging to the lower oceanic crust of the Limousin ophiolite, underwent a nearly isothermal burial to 800 °C, 10 kbar, at the boundary between the amphibolite and granulite facies conditions. The transition from the HT-LP magmatic conditions, to those of recrystallization in the upper amphibolite facies followed by retrogression at 630–670 °C, 6 ± 2 kbar, defines an isothermal pressure increase followed by an anticlockwise retrogressive P - T path (Fig. 11).

High-Al amphibolites (former troctolites or anorthositic gabbros) belonging to high-pressure or high-temperature terranes are widespread around the world but the tectonic interpretation of the metamorphic event differs largely from one occurrence to another. Similar mineral associations, P - T conditions and P - T paths are observed in HT to UHT granulites from Precambrian cratons (Santosh & Sajeew, 2006; Brandt *et al.*, 2007), in granulitic units within orogenic belts (Gibson, 1979; Gil Ibarra *et al.*, 1991) and in eclogites that underwent granulite facies P - T conditions during their exhumation (O'Brien & Vrana, 1995; Liati & Seidel, 1996). In oceanic settings, sapphirine- and/or corundum-bearing ultrabasic to basic rocks can be formed in over-thickened oceanic crust (Ishiwatari, 1985), at the lower most levels of oceanic plateaux (Grégoire *et al.*, 1994, 1998) or during subsequent subduction of the granulite facies lower crust (Tsujimori & Liou, 2004). The metamorphic sole of some ophiolites is also characterized by the presence of high-Al amphibolites that underwent similar P - T evolution (Gnos & Kurz, 1994; Tenthorey *et al.*, 1996; Garcia *et al.*, 1999; Searle & Cox, 2002; Pamir *et al.*, 2002; Operta *et al.*, 2003; Robertson *et al.*, 2009; see Fig. 11). In the Horoman peridotite (which is an ascended oceanic mantle diapir, not an ophiolite), corundum was formed in interlayered plagioclase-rich mafic rocks during subduction of the hot exhumed peridotite body (see Morishita *et al.*, 2004).

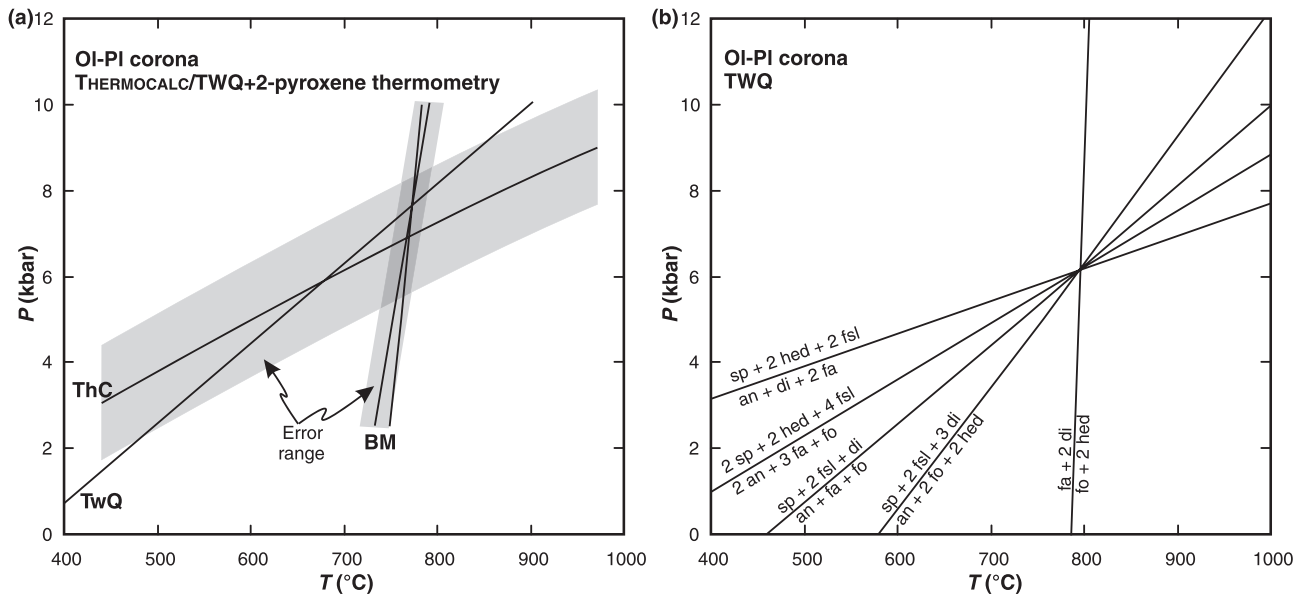


Fig. 7. Estimation of P - T conditions for the different metamorphic stages: (a) olivine-plagioclase coronae with THERMOCALC (ThC) and TWQ [modelling of reaction (1)] and two-pyroxene thermometry (BM). (b) multi-equilibrium thermobarometry of two-pyroxene-spinel coronae with TWQ.

However, the Limousin ophiolites are former oceanic rocks crystallized at LP in the lowermost section of a thin oceanic crust (Dubuisson *et al.*, 1989; Berger *et al.*, 2006) that did not undergo recrystallization in the eclogite and HT-HP granulite facies conditions before or after the HT amphibolite stage. The only explanation left to reach such high pressure conditions at constant temperature (~ 800 °C) involves the subduction of a very young and hot oceanic slab, close to a MOR. Numerical modelling of ridge subduction (Iwamori, 2000; Uehara & Aoya, 2005) indeed shows that these peculiar P - T paths and conditions can be reached during burial of a very young oceanic lithosphere. Accordingly, similar P - T conditions and/or mineral associations have been deduced for ophiolitic and associated rocks. The best example is from the Appalachian Variscan belt, where exactly the same metamorphic evolution has been deduced for metatrolites belonging to ophiolitic bodies (Tenthorey *et al.*, 1996; Peterson *et al.*, 2009). Tenthorey *et al.* (1996) have interpreted the change from 800 °C/2 kbar to 850 °C/10 kbar as a result of burial of oceanic units during continental collision, but a more recent interpretation suggests rapid subduction to 30 km depth of still hot oceanic ridge to form the amphibolites (Peterson *et al.*, 2009). In Oman, the metamorphic sole of the ophiolite comprises granulites and amphibolites that underwent similar P - T conditions (Gnos & Kurz, 1994; Searle & Cox, 2002). The authors relate this metamorphic event to subduction of passive margin rocks under a still-hot oceanic lithosphere. In the Cenozoic belt of the Balkans, the same rock associations (corundum amphibolites) are

observed in the metamorphic basement of the Tethyan ophiolites (Pamić *et al.*, 2002; Operta *et al.*, 2003; Robertson *et al.*, 2009) and the P - T evolution (peak conditions at 830 °C, 10 kbar) is interpreted as a result of concomitant subduction-obduction of oceanic lithosphere fragments. All these models suggest a subduction shortly after the formation of the oceanic crust and close to a ridge, in agreement with our proposed ridge subduction event to account for the formation of corundum-kyanite-sapphirine amphibolites in the Limousin ophiolite.

Effects of temperature, fluids and element mobility

Most troctolites and gabbros/amphibolites from the Limousin ophiolite do not display evidence for recrystallization at 800 °C and 10 kbar. Some olivine-rich troctolites only show the development of two-pyroxene-spinel coronae between olivine and plagioclase and a few gabbros show anorthite-pargasite intergrowths between low-pressure Mg-hornblende and intermediate plagioclase (Berger *et al.*, 2005). This last textural evidence clearly demonstrates that the pargasite development post-dates a former LP oceanic hydrothermal event. Gabbros with preserved magmatic textures and mineral compositions (Dubuisson *et al.*, 1989; Berger *et al.*, 2006) are also found together with typical oceanic hydrothermal rocks (epidosites, Ca-Al-rich metabasic rocks with prehnite and hydrogarnet, Berger *et al.*, 2005). Two ambiguities consequently result from these considerations: (i) despite burial of oceanic lithosphere to 30 km depth, most rocks did not register or were only slightly

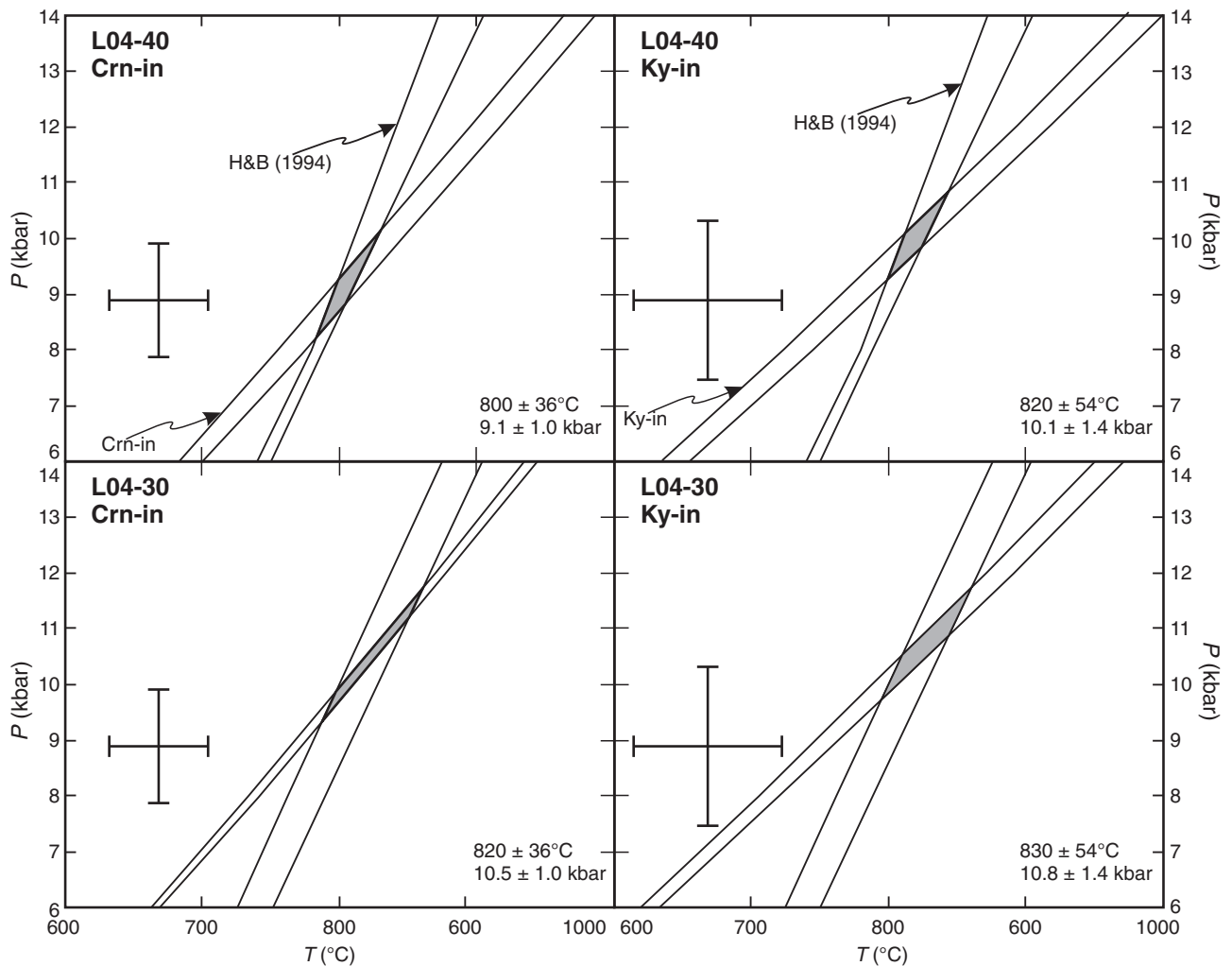


Fig. 8. Calculations of P - T conditions for corundum- and kyanite-forming reactions, samples L04-30 and L04-40. Corundum-in and kyanite-in curves are calculated with THERMOCALC, the curve labelled 'H&B (1994)' is the result of the plagioclase-amphibole thermometer of Holland & Blundy (1994) applied to plagioclase amphibole pairs in close association with corundum or kyanite. See text for detailed explanations.

affected by high-grade metamorphic reactions; (ii) some lithologies from the oceanic crust have cooled to greenschist facies conditions before the subduction event whereas metatroctolites were subducted when they were still hot, i.e. at near solidus conditions.

First, this means that a thermal gradient existed in the oceanic crust. Co-existence of hot mafic-ultramafic rocks near the crust-to-mantle transition and cooled hydrothermally-altered basic rocks close to a mid-oceanic ridge is supported by the fact that magma fluxes from the mantle are not constant, especially in slow-spreading oceans, and that fresh and hot magma can intrude already cooled oceanic rocks and supply heat to overlying hydrothermal systems (see for example, Singh *et al.*, 2006). Second, the presence of pargasite-corundum veins in coronitic troctolites (see Fig. 4) and the partial transfor-

mation of surrounding rock in pargasite-plagioclase associations prove that the pargasite-forming reactions were probably enhanced by fluid infiltration into hot troctolites at 30 km depth. Accordingly, corundum amphibolites are slightly enriched in Ca and Al compared with host troctolites, elements that are easily transported by HT fluids. Two main factors thus control the onset of metamorphic reactions to form corundum amphibolites from troctolites: the fossil temperature profile in the oceanic crust and the local infiltration of H_2O -Ca-Al-rich fluids. Preservation of hydrous, LP oceanic lithologies (mainly amphibolitized gabbros) is probably the result of incomplete reequilibration in the absence of fluid originating from a HT vein. Moreover, the maximum P - T conditions recorded by the corundum amphibolites did not reach the amphibole-out

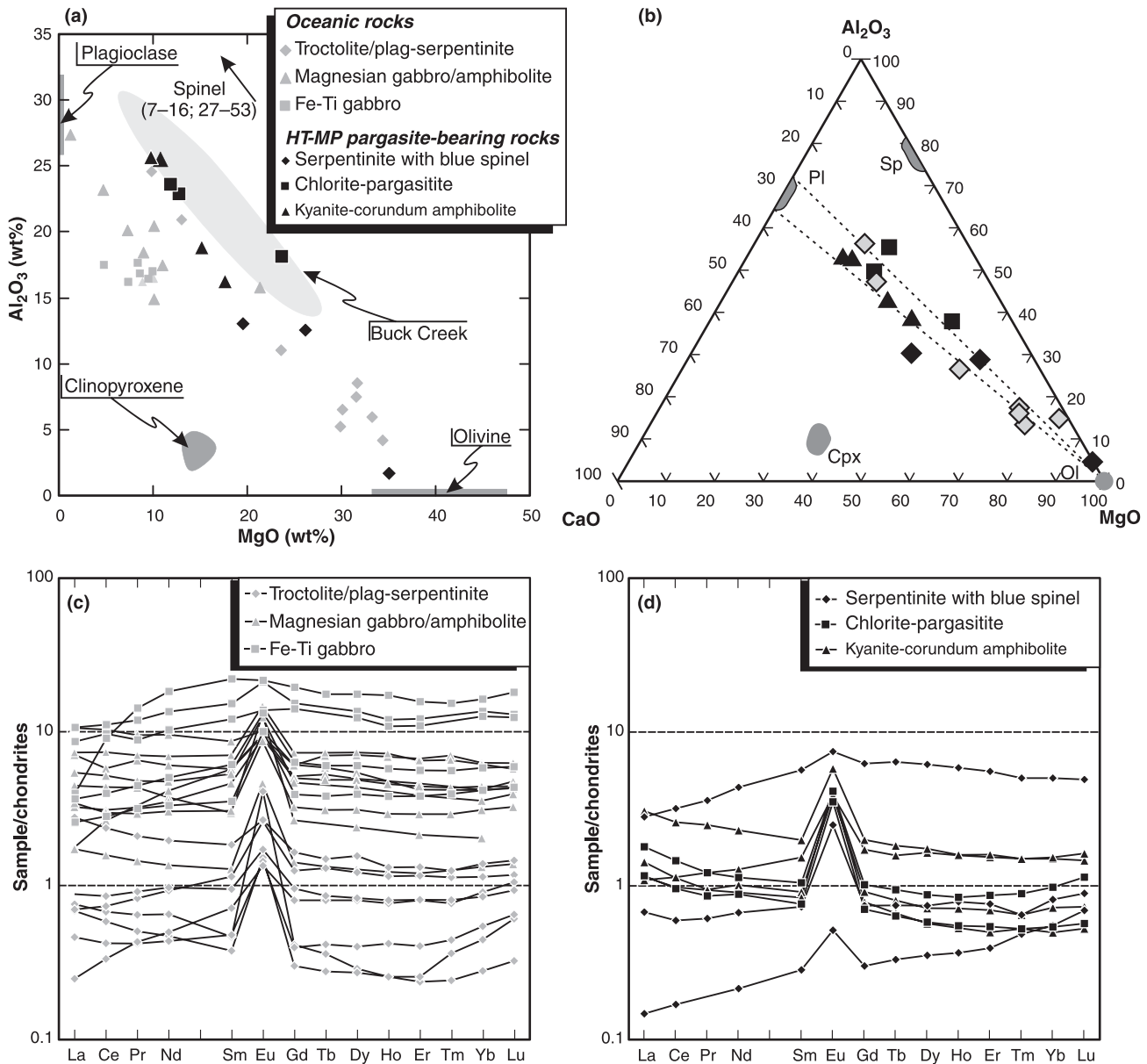


Fig. 9. Whole-rock geochemistry of the Limousin ophiolite samples: (a) binary Al_2O_3 - MgO plot of all the crustal rock types of the Limousin ophiolite; (b) triangular CaO - Al_2O_3 - MgO plot comparing the composition of corundum amphibolites and related rocks to preserved troctolites. The composition of the main primary minerals (plagioclase, olivine, clinopyroxene and spinel) is also shown; REE patterns of magmatic rocks (c) and of corundum-bearing amphibolites and related rocks (d). Normalization values from McDonough & Sun (1995).

reaction for metabasites (above 800 °C at moderate to high pressure, Pattison, 2003), thus preventing the dehydration of surrounding amphibolitized gabbros.

It is worth noting that the preservation of oceanic lithologies after a high-grade metamorphic event is not uncommon in ophiolites. One of the best examples is the Zermatt-Saas alpine ophiolite, which has been subducted to near UHP conditions (20–23 kbar, Angiboust *et al.*, 2009), but where oceanic hydrothermal mineral associations and textures are still locally

preserved (Barnicoat & Bowtell, 1995; Barnicoat & Cartwright, 1997; Li *et al.*, 2004).

Kyanite and sapphirine growth is not fully explained by isochemical reactions between the main constituents of corundum amphibolites in response to progressive evolution of *P-T* conditions. Reaction textures are indeed not observed and gedrite [one reactant in reactions (3) and (4)] is not always present in the vicinity of sapphirine and kyanite. Moreover, the *P-T* conditions for the formation of corundum, kyanite and

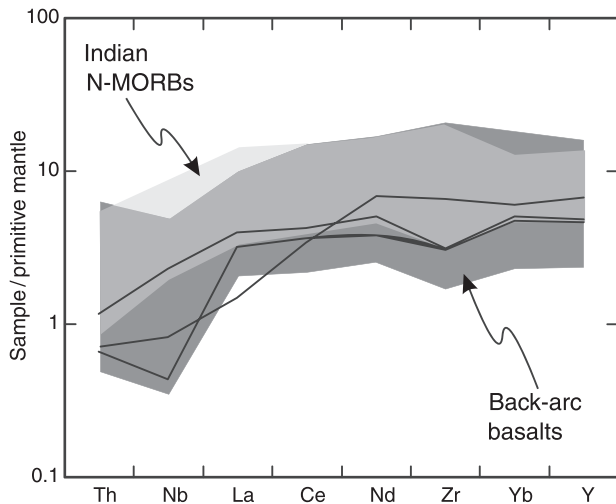


Fig. 10. Immobile trace-element patterns of high-Ti fine-grained amphibolites from the Limousin ophiolite compared with Indian-Ocean N-MORBs and back-arc basin basalts (data from the online *PETDB* database). Normalization values from McDonough & Sun (1995).

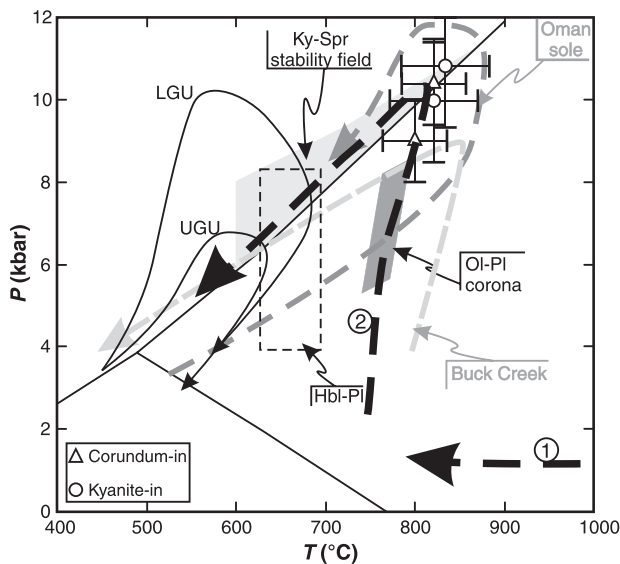


Fig. 11. Proposed P - T path (black arrows) followed by the corundum amphibolites (metatroctolites) from Limousin compared with those for the Buck-Creek ophiolitic meta-troctolites (Tenthorey *et al.*, 1996) and for the amphibolites from the metamorphic sole of the Oman Semail ophiolite (Searle & Cox, 2002): (1) Cooling of troctolites crystallized in the oceanic crust; (2) burial of hot troctolites by ridge subduction to form corundum amphibolites followed by exhumation. Sapphirine-kyanite stability field from Podlesskii *et al.* (2008). Ol-Pl: P - T range for two-pyroxene-spinel coronae formation between olivine and plagioclase (Fig. 7); Crn-in and Ky-in P - T , see Fig. 8; Hbl-Pl: P - T ranges calculated for retrogressive Mg-hornblende-plagioclase pairs in corundum amphibolites (this study). UGU (Upper Gneiss Unit) and LGU (Lower Gneiss Unit) P - T paths are from Bellot & Roig (2007).

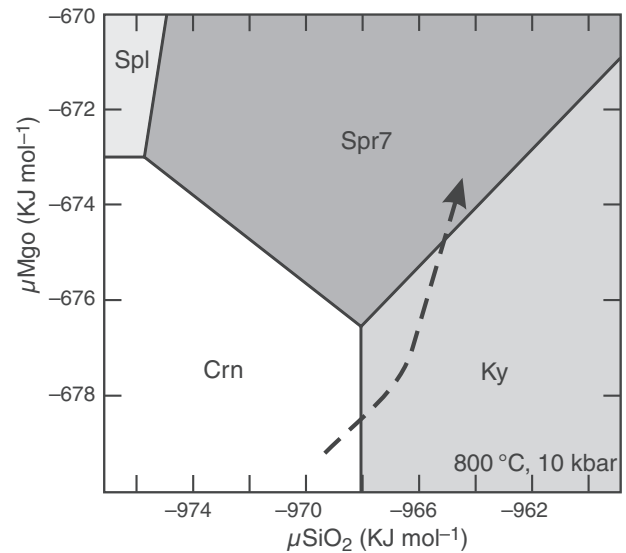


Fig. 12. μMgO - μSiO_2 diagram constructed through THERMOCALC (see White *et al.*, 2008 for detailed explanations).

sapphirine are equivalent within error ranges for the different mineral-forming reactions (780–830 °C, ~10 kbar), and the change in P - T conditions may therefore not be responsible for the onset of kyanite and sapphirine growth. The possible consequence of local MgO and SiO₂ influx has been explored using a μMgO - μSiO_2 diagram constructed in the MAS system with THERMOCALC (see White *et al.*, 2008, for detailed explanations), for P - T conditions fixed at 800 °C, 10 kbar (Fig. 12). An increase in chemical potential of these two components at fixed P - T conditions can also explain the progressive transformation of corundum into kyanite, and the transformation of kyanite into sapphirine. Mobility of MgO and SiO₂ can be enhanced by diffusion in response to small-scale chemical gradients within the rocks (corundum-kyanite-sapphirine associations are most of the time enclosed in polygonal plagioclase patches, and consequently, no MgO is available at a local scale). MgO and SiO₂ can also be transported by intergranular fluids during infiltration metasomatism. Raith *et al.* (2008) have suggested this process for the growth of spinel and sapphirine around corundum from sakeenites (corundum-spinel-sapphirine anorthitic rocks); in this case, infiltration of fluids transporting MgO and SiO₂ would be responsible for a part of the mineralogical evolution at fixed P - T conditions.

Geodynamic implications

At the scale of the whole FMC, these corundum-bearing amphibolites are always associated with metabasic rocks typical of oceanic and subduction setting (spinel-serpentinites, flaser-gabbros, eclogites and garnet granulites). As observed by Dubuisson

et al. (1988) and as in the Variscan South Armorican domain (Ballèvre *et al.*, 2009), the whole sequence made of a thin ophiolitic unit with underlying mica-schists, mafic granulites and eclogites (namely, the Middle Allochthon) shows very different lithological, structural and metamorphic features with a contrasted P – T evolution (see Fig. 11) relative to those of the Upper Allochthon (UGU) and of the Lower Allochthon (LGU). It can therefore be identified as an independent suture-zone oceanic unit. Accordingly, in other worldwide belts, such tectonic units are commonly present at the suture zone between formerly separate continental domains. In the Himalaya belt, the Indus–Tsangpo suture zone, separating the India and Tibet continental domains, comprises ophiolitic rocks (Sachan, 2001) closely associated with high-pressure eclogites, blueschists and micaschists (see Guillot *et al.*, 2008). In West Africa as well, the eastern suture of the West African craton is made of serpentinites and ocean-derived metabasic rocks, HP–UHP eclogites and blueschists, kyanite micaschists and garnet granulites (Caby, 1994; Caby *et al.*, 2008).

Due to a lack of geochronological studies on this oceanic unit in the FMC, it is difficult to reconstruct its geodynamic evolution. It is clear that a small oceanic domain was spreading, either during the Cambro–Ordovician period (at the same time as the Chamrousse SSZ oceanic crust formed; Ménot *et al.*, 1988) or during Late Devonian (development of small oceanic basins and subduction of oceanic crust during Late Devonian to Early Carboniferous; Pin, 1990; Ballèvre *et al.*, 2009). However, the structure and the small size of the oceanic basin represented by the Limousin ophiolite are more comparable with Late Devonian oceanic relics (Berger *et al.*, 2006). According to proposed geodynamic reconstructions (Matte, 2001), to palynspatic studies (von Raumer *et al.*, 2003; von Raumer & Stampfli, 2008) and to the position of Central Limousin in the prolongation of the South Armorican Suture Zone (Ballèvre *et al.*, 2009), the Limousin ocean could either correspond to the Galicia–South Brittany ocean of Matte (2001), to the Palaeo-Tethys of von Raumer *et al.* (2003) or could be a lateral equivalent of the Chamrousse ophiolite (von Raumer & Stampfli, 2008).

The whole structure and the mineralogy of the Limousin ophiolite are typical of an oceanic lithosphere formed in a MOR environment (Berger *et al.*, 2006) and some fine-grained amphibolites with melt-like geochemical fingerprints are close to N-MORBs. The ocean represented by this ophiolite has been initiated at a MOR, not in a back arc setting. However, the presence of some high-Ti amphibolites showing trace-element patterns similar to those of back-arc basin basalts suggests that the Limousin ocean floor was subjected to an intraoceanic subduction which developed supra-subduction-type magmas. The absence of voluminous island-arc magmas and/or massifs seems to suggest that this intraoceanic

subduction event was short-lived and rapidly followed by the closure of the oceanic domains (e.g. O'Brien, 2001). The mixed MOR–SSZ Limousin mid-oceanic ridge lithosphere was afterwards subducted to a maximum depth of 30 km (allowing formation of the corundum-bearing amphibolites) and then stacked between two different continental domains (the Lower and Upper Allochthons) during collision. The model of Pin & Paquette (2002) also suggests spreading of a MOR-type ocean, followed by an intraoceanic subduction and a final collision of continental domains after subduction polarity inversion during a period of quiescence in terms of tectono-sedimentary events. It is nevertheless still difficult to reconcile both models due to the lack of studies on the ophiolite-bearing unit and the absence of geochronological data for both the underlying eclogites (work in progress) and the ophiolitic rocks (only irrelevant or biased ages so far; Lafon, 1986).

CONCLUSIONS

Corundum amphibolites from the FMC formed during subduction to 30 km depth of the MOR, which accreted the Limousin ophiolite. They represent the transformation product of plagioclase-rich troctolites of this ophiolite. The close association of basic rocks characterized by preserved oceanic features with high-grade corundum amphibolites and the presence of corundum–spinel–pargasite veins in troctolites strongly support the idea that the fossil temperature profile in the former oceanic crust and the local infiltration of Ca–Al-rich aqueous fluids were determinant in the formation of high-Al amphibolites. Kyanite and sapphirine-forming reactions are not satisfactorily explained by solid-state isochemical reactions. The variations in chemical potential of MgO and SiO₂ components, in response to infiltration metasomatism and/or local scale diffusion, were probably essential to enhance growth of sapphirine and kyanite around corundum.

Such a P – T evolution involving metatroctolites is common in suture zones with an identified ophiolite, and characterizes the most famous ophiolitic complexes across the world (Oman and other Mesozoic Tethyan ophiolites; Appalachian ophiolites). The presence of the corundum–kyanite–sapphirine assemblage in the ophiolitic bodies is not in contradiction with their oceanic origin as attested by Santallier (1994) and references therein.

The oceanic domain represented by the Limousin ophiolite was initiated at a slow-spreading MOR and then subjected to intraoceanic subduction, as attested by the presence of a few SSZ-derived metabasic rocks within the MOR ophiolite. Convergence of continental domains on both sides of the ocean led to the subduction of the mixed MOR–SSZ mid-oceanic ridge and to the formation and exhumation of a suite of high-grade metabasic rocks (eclogites and granulites)

now forming a major transported tectonic suture zone stacked between the two main lithotectonic units of the FMC.

ACKNOWLEDGEMENTS

Geological mapping in the Central Limousin suture zone and whole-rock analyses have been partly financed by a BRGM Grant. F. Colleoni and T. Ronsin (former students at the University of La Rochelle, France) have productively contributed to fieldwork and mapping. The authors, and especially JCCM, want to pay a sincere tribute to D. Santallier (deceased in June 2009) for her extensive work on French Massif Central metabasic rocks and for the stimulating and fruitful discussions that helped understanding the evolution of Limousin mafic-ultramafic massifs. The two reviewers (S. Baba and T Tsujimori) and the editor (D. Robinson) are thanked for their critical comments and their suggestions that contributed to the improvement of the paper.

REFERENCES

- Alexandrov, P., Floc'h, J.P., Cuney, M. & Cheilletz, A., 2001. Ionic microprobe dating of zircons from the Upper Gneiss Unit (South Limousin, Massif Central, France). *Comptes Rendus de l'Académie des Sciences*, **332**, 625–632.
- Angiboust, S., Agard, P., Jolivet, L. & Beyssac, O., 2009. The Zermatt-Saas ophiolite: the largest (60-km wide) and deepest (c. 70–80 km) continuous slice of oceanic lithosphere detached from a subduction zone?. *Terra Nova*, **21**, 171–180.
- Ballèvre, M., Bosse, V., Ducassou, C. & Pitra, P., 2009. Palaeozoic history of the Armorican Massif: models for the tectonic evolution of the suture zones. *Comptes Rendus Géoscience*, **341**, 174–201.
- Barnicoat, A.C. & Bowtell, S.A., 1995. Sea-floor hydrothermal alteration in metabasites from high-pressure ophiolites of the Zermatt-Aosta area of the western Alps. *Museo Regionale di Scienze Naturali di Torino, Bollettino*, **13**, 191–220.
- Barnicoat, A.C. & Cartwright, I., 1997. The gabbro-eclogite transformation: an oxygen isotope and petrographic study of west Alpine ophiolites. *Journal of Metamorphic Geology*, **15**, 93–104.
- Bellet, J.P. & Roig, J.Y., 2007. Episodic exhumation of HP rocks inferred from structural data and *P-T* paths from the Southwestern Massif Central (Variscan belt, France). *Journal of Structural Geology*, **29**, 1538–1557.
- Berger, J., Féménias, O., Mercier, J.-C.C. & Demaiffe, D., 2005. Ocean-floor hydrothermal metamorphism in the Limousin ophiolites (western French Massif Central): evidence of a rare preserved Variscan oceanic marker. *Journal of Metamorphic Geology*, **23**, 795–812.
- Berger, J., Féménias, O., Mercier, J.-C.C. & Demaiffe, D., 2006. A Variscan slow-spreading ridge (MOR-LHOT) in Limousin (French Massif Central): magmatic evolution and tectonic setting inferred from mineral chemistry. *Mineralogical Magazine*, **70**, 175–185.
- Berman, R.G., 1988. Internally-consistent thermodynamic data for minerals in the system $\text{Na}_2\text{O}-\text{K}_2\text{O}-\text{CaO}-\text{MgO}-\text{FeO}-\text{Fe}_2\text{O}_3-\text{Al}_2\text{O}_3-\text{SiO}_2-\text{TiO}_2-\text{H}_2\text{O}-\text{CO}_2$. *Journal of Petrology*, **29**, 445–522.
- Bertrand, P. & Mercier, J.-C.C., 1985. The mutual solubility of coexisting ortho- and clinopyroxene; toward an absolute geothermometer for the natural system? *Earth and Planetary Science Letters*, **76**, 109–122.
- Brandt, S., Will, T.M. & Klemd, R., 2007. Magmatic loading in the Proterozoic Epupa Complex, NW Namibia, as evidenced by ultrahigh-temperature sapphirine-bearing orthopyroxene-sillimanite-quartz granulites. *Precambrian Research*, **153**, 143–178.
- Briand, B., Chenevoy, M., Chamayou, J., Guyonnaud, G. & Recoing, M., 1982. *Notice explicative et carte géologique de France au 1:50.000, feuille Châlus*. BRGM, Orléans.
- Caby, R., 1994. Precambrian coesite from Northern Mali – 1st record and implications for plate-tectonics in the Trans-Saharan segment of the Pan-African Belt. *European Journal of Mineralogy*, **6**, 235–244.
- Caby, R., Buscaïl, F., Demebele, D., Diakite, S., Sacko, S. & Bal, M., 2008. Neoproterozoic garnet-glaucophanites and eclogites: new insights for subduction metamorphism of the Gourma fold and thrust belt (eastern Mali). *Geological Society of London, Special Publications*, **297**, 203–216.
- Carignan, J., Hild, P., Mévelle, G., Morel, J. & Yeghicheyan, D., 2001. Routine analyses of trace elements in geological samples using flow injection and low pressure on-line liquid chromatography coupled to ICP-MS: a study of geochemical reference materials BR, DR-N, UB-N, AN-G and GH. *Geostandards Newsletter*, **25**, 187–198.
- Chenevoy, M., Delbos, R. & Vautrelle, C., 1990. *Notice explicative et carte géologique de France au 1:50.000, feuille Nexon*. BRGM, Orléans.
- Dale, J., Powell, R., White, R.W., Elmer, F.L. & Holland, T.J.B., 2005. A thermodynamic model for Ca-Na clinopyroxenes in $\text{Na}_2\text{O}-\text{CaO}-\text{FeO}-\text{MgO}-\text{Al}_2\text{O}_3-\text{SiO}_2-\text{H}_2\text{O}-\text{O}$ for petrological calculations. *Journal of Metamorphic Geology*, **23**, 771–791.
- Dilek, Y., Furnes, H. & Shallo, M., 2008. Geochemistry of the Jurassic Mirdita Ophiolite (Albania) and the MORB to SSZ evolution of a marginal basin oceanic crust. *Lithos*, **100**, 174–209.
- Dubuisson, G., Hirn, A., Girardeau, J., Mercier, J.C.C. & Veinante, J.L., 1988. Multiple Variscan nappes in Limousin, Western Massif Central, France – geophysical constraints to the geological model and geodynamic implications. *Tectonophysics*, **147**, 19–31.
- Dubuisson, G., Mercier, J.-C.C., Girardeau, J. & Frison, J.Y., 1989. Evidence for a lost ocean in Variscan terranes of the Western Massif Central, France. *Nature*, **337**, 729–732.
- Faure, M., Lardeaux, J.M. & Ledru, P., 2009. A review of the pre-Permian geology of the Variscan French Massif Central. *Comptes Rendus Géoscience*, **341**, 202–213.
- Floc'h, J.-P., Guillot, P.-L., Platel, J.-P. et al., 1979. *Notice explicative et carte géologique de France au 1:50.000, feuille Thiviers*. BRGM, Orléans.
- Forestier, F.H. & Lasnier, B., 1969. Découverte de niveaux d'amphibolites à pargasite, anorthite, corindon et sapphirine dans les schistes cristallins de la vallée du Haut-Allier; existence du faciès granulite dans le Massif Central Français. *Contributions to Mineralogy and Petrology*, **23**, 194–235.
- García, F.D., Arenas, R., Catalan, J.R.M., del Tanago, J.G. & Dunning, G.R., 1999. Tectonic evolution of the Careon ophiolite (northwest Spain). A remnant of oceanic lithosphere in the Variscan belt. *Journal of Geology*, **107**, 587–605.
- García-Casco, A., Lazaro, C., Rojas-Agramonte, Y. et al., 2008. Partial melting and counterclockwise *P-T* path of subducted oceanic crust (Sierra del Convento Melange, Cuba). *Journal of Petrology*, **49**, 129–161.
- Gibson, G.M., 1979. Margarite in kyanite- and corundum-bearing anorthosite, amphibolite, and hornblende from Central Fiordland, New Zealand. *Contributions to Mineralogy and Petrology*, **68**, 171–179.
- Gil Ibarra, J.I., Mendia, M. & Girardeau, J., 1991. Mg-rich and Cr-rich staurolite and Cr-rich kyanite in high-pressure ultrabasic rocks (Cabo Ortegal, Northwestern Spain). *American Mineralogist*, **76**, 501–511.
- Glodny, J., Kuhn, A. & Austrheim, H., 2008. Geochronology of fluid-induced eclogite and amphibolite facies metamorphic

- reactions in a subduction-collision system, Bergen Arcs, Norway. *Contributions to Mineralogy and Petrology*, **156**, 27–48.
- Gnos, E. & Kurz, D., 1994. Sapphirine-quartz and sapphirine-corundum assemblages in metamorphic rocks associated with the Semail Ophiolite (United-Arab-Emirates). *Contributions to Mineralogy and Petrology*, **116**, 398–410.
- Godard, G., 1990. Discovery of eclogites, spinel-bearing peridotites and anorthite, spinel and corundum-bearing amphibolites in the Morvan, NE French Massif Central. *Comptes Rendus de l'Académie des Sciences*, **310**, 227–232.
- Grégoire, M., Mattielli, N., Nicollet, C. *et al.*, 1994. Oceanic mafic granulite xenoliths from the Kerguelen archipelago. *Nature*, **367**, 360–363.
- Grégoire, M., Cottin, J.Y., Giret, A., Mattielli, N. & Weis, D., 1998. The meta-igneous granulite xenoliths from Kerguelen Archipelago: evidence of a continent nucleation in an oceanic setting. *Contributions to Mineralogy and Petrology*, **133**, 259–283.
- Guillot, S., Maheo, G., de Sigoyer, J., Hattori, K.H. & Pecher, A., 2008. Tethyan and Indian subduction viewed from the Himalayan high- to ultrahigh-pressure metamorphic rocks. *Tectonophysics*, **451**, 225–241.
- Holland, T. & Blundy, J., 1994. Nonideal interactions in calcic amphiboles and their bearing on amphibole-plagioclase thermometry. *Contributions to Mineralogy and Petrology*, **116**, 433–447.
- Holland, T.J.B. & Powell, R., 1998. An internally consistent thermodynamic data set for phases of petrological interest. *Journal of Metamorphic Geology*, **16**, 309–343.
- Ishiwatari, A., 1985. Granulite-facies metacumulates of the Yakuno ophiolite, Japan: evidence for unusually thick oceanic crust. *Journal of Petrology*, **26**, 1–30.
- Iwamori, H., 2000. Thermal effects of ridge subduction and its implications for the origin of granitic batholith and paired metamorphic belts. *Earth and Planetary Science Letters*, **181**, 131–144.
- Lafon, J.M., 1986. *Géochronologie U-Pb appliquée à deux segments du Massif Central français: Le Rouergue oriental et le Limousin central*. Unpublished PhD thesis, Montpellier, France, 152 pp.
- Lasnier, B. & Marchand, D., 1979. *Notice explicative et carte géologique de France au 1:50.000, feuille Brioude*. BRGM, Orléans.
- Leake, B.E., Woolley, A.R., Birch, W.D. *et al.*, 1997. Nomenclature of amphiboles – report of the subcommittee on Amphiboles of the International Mineralogical Association Commission on New Minerals and Mineral Names. *European Journal of Mineralogy*, **9**, 623–651.
- Li, X.P., Rahn, M. & Bucher, K., 2004. Serpentinites of the Zermatt-Saas ophiolite complex and their texture evolution. *Journal of Metamorphic Geology*, **22**, 159–177.
- Liati, A. & Seidel, E., 1996. Metamorphic evolution and geochemistry of kyanite eclogites in central Rhodope, northern Greece. *Contributions to Mineralogy and Petrology*, **123**, 293–307.
- Marchand, D., Bouiller, R., Burg, J.-P. & Cornen, G., 1989. *Notice explicative et carte géologique de France au 1:50.000, feuille Langeac*. BRGM, Orléans.
- Matte, P., 2001. The Variscan collage and orogeny (480–290 Ma) and the tectonic definition of the Armorica microplate: a review. *Terra Nova*, **13**, 122–128.
- McDonough, W.F. & Sun, S.S., 1995. The composition of the Earth. *Chemical Geology*, **120**, 223–253.
- Melleton, J., Cocherie, A., Faure, M. & Rossi, P., 2009. Precambrian protoliths and Early Paleozoic magmatism in the French Massif Central: U-Pb data and the North Gondwana connection in the west European Variscan belt. *Gondwana Research*, **17**, 13–25.
- Ménot, R. & Piboule, M., 1977. Les massifs basiques et ultrabasiques antemetamorphiques de la région de Chalus, Limousin (feuille de Chalus XIX-32 a 1/50 000). *Bulletin du Bureau de Recherches Géologiques et Minières*, **4**, 307–332.
- Ménot, R.P., Peucat, J.J., Scarenzi, D. & Piboule, M., 1988. 496-My Age of plagiogranites in the Chamrousse ophiolite complex (external crystalline Massifs in the French Alps) – evidence of a Lower Paleozoic oceanization. *Earth and Planetary Science Letters*, **88**, 82–92.
- Messenier, G., Astruc, J.G., Bambier, A., Collomb, P., Galharrague, J. & Roche, J., 1984. *Notice explicative et carte géologique de France au 1:50.000, feuille Millau*. BRGM, Orléans.
- Morishita, T., Arai, S. & Green, D.H., 2004. Possible non-melted remnants of subducted lithosphere: experimental and geochemical evidence from corundum-bearing mafic rocks in the Horoman peridotite complex, Japan. *Journal of Petrology*, **45**, 235–252.
- Nimis, P. & Ulmer, P., 1998. Clinopyroxene geobarometry of magmatic rocks Part 1: an expanded structural geobarometer for anhydrous and hydrous, basic and ultrabasic systems. *Contributions to Mineralogy and Petrology*, **133**, 122–135.
- O'Brien, P.J., 2001. Subduction followed by collision: alpine and Himalayan examples. *Physics of the Earth and Planetary Interiors*, **127**, 277–291.
- O'Brien, P.J. & Vrana, S., 1995. Eclogites with a short-lived granulite-facies overprint in the Moldanubian Zone, Czech Republic – petrology, geochemistry and diffusion modeling of garnet zoning. *Geologische Rundschau*, **84**, 473–488.
- Ohnenstetter, M., 1994. Devonian ophiolites, Eastern Massif Central. In: *Pre-Mesozoic Geology in France and Related Areas* (ed. Keppie, J.D.), pp. 358–363. Springer Verlag, Berlin.
- Operta, M., Pamic, J., Balen, D. & Tropper, P., 2003. Corundum-bearing amphibolites from the metamorphic basement of the Krivaja-Konjuh ultramafic massif (Dinaride Ophiolite Zone, Bosnia). *Mineralogy and Petrology*, **77**, 287–295.
- Otten, M.T., 1984. Na-Al-rich gedrite coexisting with hornblende in a corona between plagioclase and olivine. *American Mineralogist*, **69**, 458–464.
- Pamic, J., Tomljenovic, B. & Balen, D., 2002. Geodynamic and petrogenetic evolution of Alpine ophiolites from the central and NW Dinarides: an overview. *Lithos*, **65**, 113–142.
- Pattison, D.R.M., 2003. Petrogenetic significance of orthopyroxene-free garnet plus clinopyroxene plus plagioclase +/- quartz-bearing metabasites with respect to the amphibolite and granulite facies. *Journal of Metamorphic Geology*, **21**, 21–34.
- Peacock, S.M., 2003. Thermal structure and metamorphic evolution of subducting slabs. In: *Inside the Subduction Factory, Geophysical Monograph* (ed. Eiler, J.), pp. 7–22. American Geophysical Union, Washington, DC.
- Peacock, S.M., Rushmer, T. & Thompson, A.B., 1994. Partial Melting of Subducting Oceanic-Crust. *Earth and Planetary Science Letters*, **121**, 227–244.
- Pearce, J.A., 2003. Supra-subduction zone ophiolites; the search for modern analogues. In: *Ophiolite Concept and the Evolution of the Geological Thought. Special Paper 373 – Geological Society of America* (eds Dilek, Y. & Newcomb, S.), pp. 269–293. Geological Society of America (GSA), Boulder, CO.
- Peterson, V., Ryan, J.G. & Program, R.E.U.S., 2009. Petrogenesis and structure of the Buck Creek mafic-ultramafic suite, southern Appalachians: constraints on ophiolite evolution and emplacement in collisional orogens. *Geological Society of America Bulletin*, **121**, 615–629.
- Piboule, M. & Ménot, R.P., 1976. Sur une paragenèse aargasite-gedrite-disthène-corindon dans les metagabbros des massifs basiques et ultrabasiques différenciés de Limousin (Massif Central français). *Comptes Rendus Hebdomadaires des Séances de l'Académie des Sciences, Série D: Sciences Naturelles*, **282**, 141–144.
- Pin, C., 1990. Variscan oceans – ages, origins and geodynamic implications inferred from geochemical and radiometric data. *Tectonophysics*, **177**, 215–227.

- Pin, C. & Paquette, J.L., 2002. Sr-Nd isotope and trace element evidence for a Late Devonian active margin in northern Massif-Central (France). *Geodinamica Acta*, **15**, 63–77.
- Podlesskii, K.K., Aranovich, L.Y., Gerya, T.V. & Kosyakova, N.A., 2008. Sapphirine-bearing assemblages in the system MgO-Al₂O₃-SiO₂: a continuing ambiguity. *European Journal of Mineralogy*, **20**, 721–734.
- Pouchou, J.L. & Pichoir, F., 1991. Quantitative analysis of homogeneous or stratified microvolumes applying the model "PAP". In: *Electron Probe Quantification* (eds Heinrich, K.J.F. & Newbury, D.E.), pp. 31–75. Plenum Press, New York.
- Powell, R. & Holland, T.J.B., 1988. An internally consistent dataset with uncertainties and correlations. 3. Applications to geobarometry, worked examples and a computer-program. *Journal of Metamorphic Geology*, **6**, 173–204.
- Raith, M.M., Rakotondrazafy, R. & Sengupta, P., 2008. Petrology of corundum-spinel-sapphirine-anorthite rocks (sakenites) from the type locality in southern Madagascar. *Journal of Metamorphic Geology*, **26**, 647–667.
- von Raumer, J.F. & Stampfli, G.M., 2008. The birth of the Rhenic Ocean–Early Palaeozoic subsidence patterns and subsequent tectonic plate scenarios. *Tectonophysics*, **461**, 9–20.
- von Raumer, J.F., Stampfli, G.A. & Bussy, F., 2003. Gondwana-derived microcontinents – the constituents of the Variscan and Alpine collisional orogens. *Tectonophysics*, **365**, 7–22.
- Robertson, A., Karamata, S. & Saric, K., 2009. Overview of ophiolites and related units in the Late Palaeozoic–Early Cenozoic magmatic and tectonic development of Tethys in the northern part of the Balkan region. *Lithos*, **108**, 1–36.
- de Ronde, A.A. & Stunitz, H., 2007. Deformation-enhanced reaction in experimentally deformed plagioclase-olivine aggregates. *Contributions to Mineralogy and Petrology*, **153**, 699–717.
- Rubie, D.C., 1986. The catalysis of mineral reactions by water and restrictions on the presence of aqueous fluid during metamorphism. *Mineralogical Magazine*, **50**, 399–415.
- Sachan, H.K., 2001. Supra-subduction origin of the Nidar ophiolitic sequence, Indus Suture Zone, Ladakh, India: evidence from mineral chemistry of upper mantle rocks. *Ophioliti*, **26**, 23–32.
- Santallier, D., 1994. A Reply: another way of considering the Ophiolite question, In: *Pre-Mesozoic Geology in France and Related Areas*. (ed. Keppie, J.D.), pp. 354–358. Springer Verlag, Berlin.
- Santosh, M. & Sajeed, K., 2006. Anticlockwise evolution of ultrahigh-temperature granulites within continental collision zone in southern India. *Lithos*, **92**, 447–464.
- Sato, K., Miyamoto, T. & Kawasaki, T., 2006. Experimental calibration of sapphirine-spinel Fe²⁺-Mg exchange thermometer: implication for constraints on *P-T* condition of Howard Hills, Napier Complex, East Antarctica. *Gondwana Research*, **9**, 398–408.
- Schmidt, M.W., 1992. Amphibole composition in tonalite as a function of pressure – an experimental calibration of the Al-in-Hornblende barometer. *Contributions to Mineralogy and Petrology*, **110**, 304–310.
- Schneider, J., Bosch, D., Monié, P. & Bruguier, O., 2007. Micro-scale element migration during eclogitization in the Bergen arcs (Norway): a case study on the role of fluids and deformation. *Lithos*, **96**, 325–352.
- Searle, M.P. & Cox, J., 2002. Subduction zone metamorphism during formation and emplacement of the Semail ophiolite in the Oman Mountains. *Geological Magazine*, **139**, 241–255.
- Sider, H. & Ohnenstetter, M., 1986. Field and petrological evidence for the development of an ensialic marginal basin related to the Hercynian orogeny in the Massif Central, France. *Geologisches Rundschau*, **75**, 421–443.
- Singh, S.C., Crawford, W.C., Carton, H. et al., 2006. Discovery of a magma chamber and faults beneath a Mid-Atlantic Ridge hydrothermal field. *Nature*, **442**, 1029–1032.
- Spear, F.S., 1993. *Metamorphic Phase Equilibria and Pressure-Temperature-Time Paths*. Mineralogical Society of America, Washington, DC, USA, 799 pp.
- Tenthorey, E.A., Ryan, J.G. & Snow, E.A., 1996. Petrogenesis of sapphirine-bearing metatrolites from the Buck Creek ultramafic body, southern Appalachians. *Journal of Metamorphic Geology*, **14**, 103–114.
- Tsujimori, T. & Liou, J.G., 2004. Metamorphic evolution of kyanite-staurolite-bearing epidote-amphibolite from the Early Palaeozoic Oeyama belt, SW Japan. *Journal of Metamorphic Geology*, **22**, 301–313.
- Uehara, S. & Aoya, M., 2005. Thermal model for approach of a spreading ridge to subduction zones and its implications for high-P/high-T metamorphism: importance of subduction versus ridge approach ratio. *Tectonics*, **24**, TC4007.
- Villiger, S., Ulmer, P., Muntener, O. & Thompson, A.B., 2004. The liquid line of descent of anhydrous, mantle-derived, tholeiitic liquids by fractional and equilibrium crystallization – an experimental study at 1.0 GPa. *Journal of Petrology*, **45**, 2369–2388.
- White, R.W., Powell, R. & Baldwin, J.A., 2008. Calculated phase equilibria involving chemical potentials to investigate the textural evolution of metamorphic rocks. *Journal of Metamorphic Geology*, **26**, 181–198.
- Will, T.M. & Powell, R., 1992. Activity-composition relationships in multicomponent amphiboles – an application of Darken Quadratic Formalism. *American Mineralogist*, **77**, 954–966.

SUPPORTING INFORMATION

Additional Supporting Information may be found in the online version of this article:

Table S1. Whole-rock major- and trace-element composition of the main rock types forming the Limousin ophiolites.

Please note: Wiley-Blackwell are not responsible for the content or functionality of any supporting materials supplied by the authors. Any queries (other than missing material) should be directed to the corresponding author for the article.

Received 13 July 2009; revision accepted 13 January 2010.